NOAA Technical Memorandum ERL WMPO-33

U.S. DEPARTMENT OF COMMERCE
NATIONAL OCEANIC AND ATMOSPHERIC ADMINISTRATION
Environmental Research Laboratories

CLOUD INTERACTION AND THE FORMATION OF THE 15 JUNE 1973 TORNADO IN THE FACE MESONETWORK

Ronald L. Holle
Michael W. Maier

Weather Modification Program Office
Miami, Florida
October 1976

NOAA Technical Memorandum ERL WMPO-33

CLOUD INTERACTION AND THE FORMATION OF THE 15 JUNE 1973 TORNADO IN THE FACE MESONETWORK

Ronald L. Holle
Michael W. Maier

National Hurricane and Experimental Meteorology Laboratory
Coral Gables, Florida

Weather Modification Program Office
Miami, Florida
October 1976

UNITED STATES
DEPARTMENT OF COMMERCE
Elliot L. Richardson, Secretary

NATIONAL OCEANIC AND
ATMOSPHERIC ADMINISTRATION
Robert M. White, Administrator

Environmental Research
Laboratories
Wilmot N. Hess, Director

CONTENTS

ILLUSTRATIONS

ILLUSTRATIONS (Continued)

TABLES

CLOUD INTERACTION AND THE FORMATION OF THE 15 JUNE 1973 TORNADO IN THE FACE MESONETWORK

Ronald L. Holle and Michael W. Maier

The 15 June 1973 tornado that occurred within the FACE surface mesonetwork was measured from a series of 15 photographs taken in the vicinity.

Very weak synoptic-scale flow was evident at all levels to 100 mb over south Florida. A weak ridge at low levels and a slight trough at 500 mb were the only significant features in the area. Normal stability for summer 1973 was found at Miami, but shear (2 m s^{-1}) was the weakest of the summer, equalled only on 16 June. Rainfall over Florida was related to heating, coastal, and lakeshore effects of the peninsula and not to external factors.

Two clouds with tops of 15.6 km reached their peak intensity 25 km east and west of the tornado 50 minutes before its start. A new cloud line rapidly formed because of surface convergence up to 2.4 x 10^{-3} s^{-1} halfway between the original clouds; the tornado dipped from this line. The radar detected significant amounts of rain at 2 km when the tornado was at its peak intensity. Five minutes later the downdraft rain reached the funnel and caused it to dissipate. Surface rain gages measured very heavy precipitation another 5 minutes later at the old tornado position.

Another tornado in Oklahoma is examined and rain shafts are seen on either side in earlier stages. This case suggests that cloud interaction in a moving squall line may be as important as that of the stationary Florida environment of 15 June.

1. INTRODUCTION

Three unique circumstances attended the occurrence of the 15 June 1973 tornado during the Florida Area Cumulus Experiment (FACE) south of Lake Okeechobee, Florida. (1) The tornado occurred within a dense wind and precipitation research network; few other tornadoes have done this. (2) It formed in a nearly calm atmosphere on the synoptic scale, rather than in the environment of rapid, complex motion that usually spawns tornadoes in higher latitudes. (3) It occurred at a convergence line caused by the meeting of the outflow from two dying thunderstorms. Because the tornado was within the mesonetwork, details of the cloud-scale, rather than large-scale, motions can be isolated as dominant.

Previous occurrences of tornadoes in research mesonetworks appear to have been limited to a pair of tornadoes in the National Severe Storms Laboratory (NSSL) network in 1970 described by Barnes (1974), another NSSL storm in

1969 studied by Lemon (1974), and six tornadoes in the Illinois State Water Survey network in 1968 (Changnon and Wilson, 1971). All of these tornadoes are of the mid-latitude type, so that the FACE vortex is the first to occur in a mesonetwork under a tropical regime. Other studies of cloud structure during severe weather have been restricted to a combination of larger scale wind networks, photographs and radar data taken during a tornado's lifetime, and damage surveys after the storm. Considerable information has been gained on tornado structure near and within the vortex by this type of data analysis, beginning with the Dallas and Fargo tornadoes examined by Hoecker et al. (1960) and Fujita (1960), and followed by numerous other studies.

Florida tornadoes have not been studied extensively because they do not cause major damage, and are of short duration. This inattention may also have occurred because they were considered weak, but structurally similar, versions of middle-latitude tornadoes. Middle-latitude tornadoes are usually parts of moving squall lines in a strongly sheared environment. Typical is the tornado outbreak of April 1974, whose synoptic features were studied by Hoxit and Chappell (1975). However, this situation is frequently not the case in Florida. In table 1, we list the general characteristics of three distinct types of tornadoes that appear in Florida, and more generally, in tropical land areas. The first category, the frontal tornado, is similar to the tornado in other parts of the United States. The hurricane-related tornado, studied by Novlan and Gray (1974), occurs only in years when tropical cyclones affect Florida. The third type, the summer tropical, will be examined by a case study given in this report.

The summer tropical tornado has neither been isolated clearly nor studied extensively in past research. The life cycle of the FACE tornado is similar in many respects to that of waterspouts described by Golden (1974) and Rossow (1970), but the FACE tornado's occurrence in the mesonet has provided surface information on structure that the waterspout studies could not measure.

Table 1. Types of tornadoes that occur in Florida

	Frontal	Hurricane	Summer tropical
Season	Winter	Summer	Summer
Annual frequency	≈15	≈3	≈18
Florida weather pattern	Front/squall line	Tropical cyclone	Weak trough or col
850-200 mb wind shear	Strong	Strong	None
Stability	Extremely unstable	Neutral	Neutral
Jet stream present	Yes	No	No
Relative intensity	Strong	Moderate	Weak
Durations	>10 minutes	<5 minutes	5 to 10 minutes
Relative path length	Long	Short	Very short

The similarity of waterspouts to the summer tropical tornado is emphasized by a case that shows the simultaneous existence of both phenomena near each other along Florida's east coast (Maier and Brandli, 1973). Gerrish (1967) and Senn, et al. (1969) have studied the characteristics of the summer tropical tornado on radar and in both the Florida and synoptic-scale flow features. They have clearly shown most of the conditions given in table 1 for this type of tornado. Radar observation of intersecting fine lines related to tornado development was made from Coral Gables by Gerrish (1969). It was suggested that the fine lines represented edges of cold downdrafts from nearby thunderstorms. Charba (1974) studied the structure of large mature outdrafts in Oklahoma and their relation to severe weather. Thunderstorm outdrafts are frequently seen in satellite data, especially since resolution has become good enough to illustrate their low-level cloud representation (Brandli and Orndorff, 1976).

The 15 June 1973 tornado appears to be similar in development to the one discussed by Gerrish; our fortuitous opportunity to observe it in a mesonet allows detailed documentation of this particular case. A better understanding of how the tornado formed by cloud interaction should be of significance in understanding more about the role of cloud interaction in other south Florida situations, and should further our understanding of natural and seeded clouds.

The FACE 1973 program was executed in the area shown in figure 1; complete data lists are given by Staff, EML (1974). A cloud seeding experiment was conducted in the largest rectangle of figure 1 during FACE. Radar coverage was provided by the digitized National Weather Service WSR-57M located in Coral Gables. Its rainfall mesurements, usually made at 0.5° elevation, were checked against the surface rain gages to adjust the radar measurements of rainfall on a daily basis. The gages were located in clusters and in a mesonetwork operated jointly by the University of Virginia and NOAA personnel (fig. 1); dual Doppler radar coverage was not yet operational on the tornado day. The following analyses use all available data on 15 June; charts range in size from the synoptic down to the meso- and tornado scales. A preliminary version of this study was published by Holle and Maier (1974).

2. THE TORNADO

On the first day of field operations during FACE 1973, a tornado that occurred in the mesonetwork was viewed and photographed from the Central Site observation station. No FACE flight operations were conducted on this day. Figure 2 shows Central Site relative to the entire network, whose polygonal boundary can be located in south Florida in figure 1. A total of 22 C-set systems recording surface rainfall, wind speed and wind direction were operated from 15 June to 15 August. On 15 June there were two inoperative stations, one at Central Site and the other in the southeast portion of the network. The authors were located at Central Site and recorded approximate wind and precipitation data from 1500 to 1600 EDT, the hour in which the tornado formed and dissipated. An additional 229 locations with daily nonrecording fencepost rain gages were situated within the mesonetwork.

The time frame of the tornado's life cycle was the following: outflows

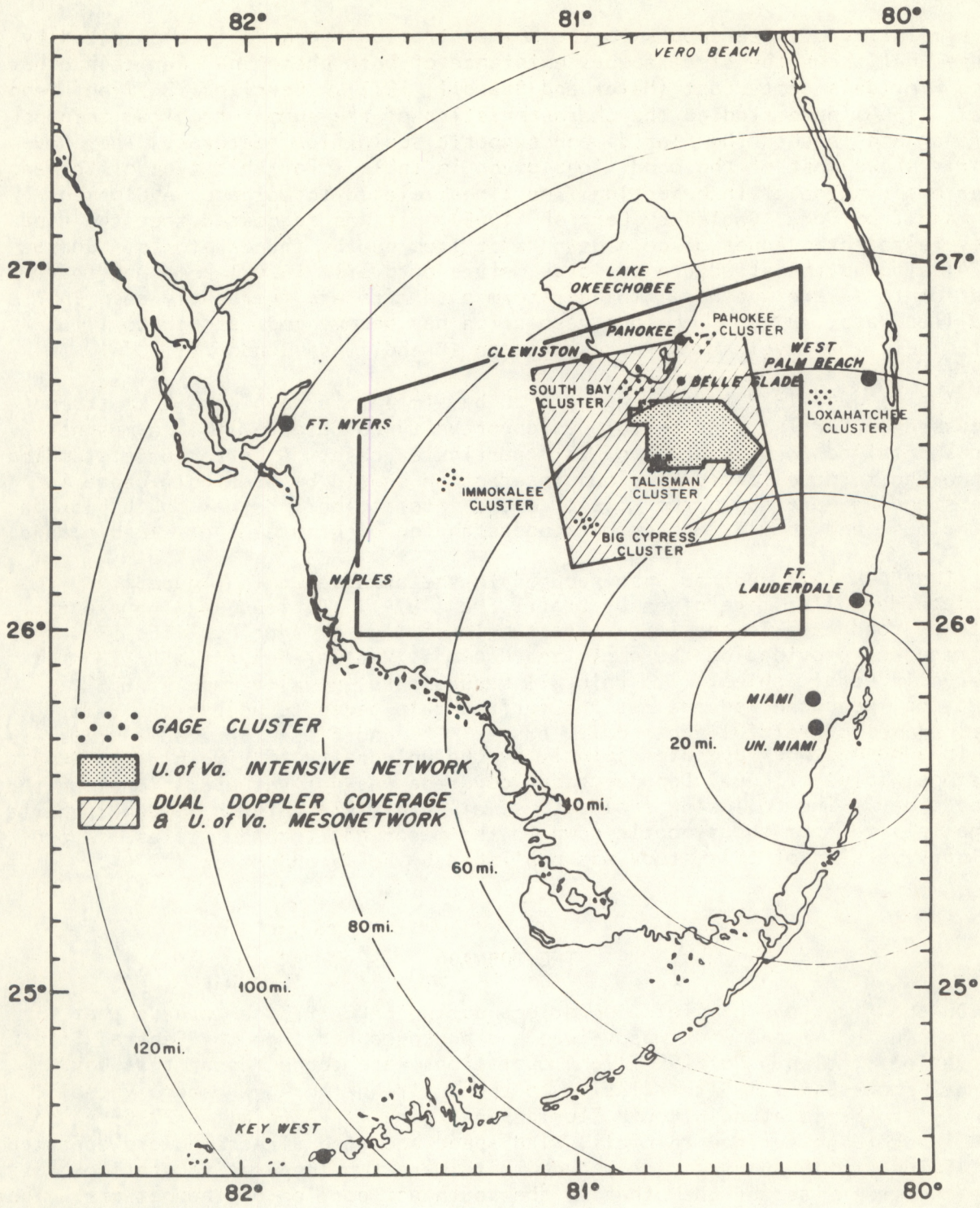

Figure 1. The FACE 1973 experimental areas. Seeding of supercooled cumuli took place within the largest rectangle. Range circles in n.mi. are from the Miami National Weather Service WSR-57M radar. The tornado occurred within the stippled intensive network on 15 June.

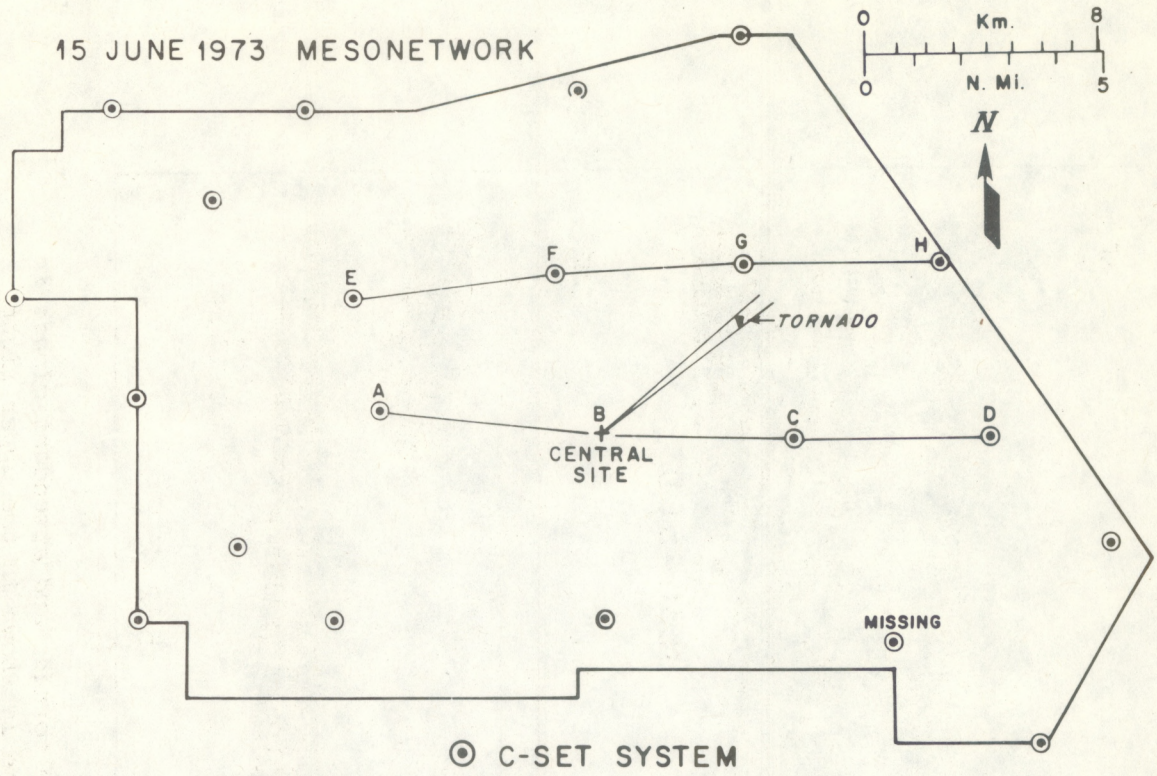

Figure 2. The mesonetwork on 15 June 1973 (its polygonal boundary is located in Florida in fig. 1). Twenty C-sets recording surface rainfall, wind speed and direction are located. The authors were at Central Site and photographed the tornado which was within the aximuths and at the distance indicated by the triangle.

from two mature thunderstorms formed a new cloud line from 1500 to 1530 EDT, the tornado was seen from 1530 to 1540, and the new cloud line grew to a mature, heavy rain stage by 1600. (In all subsequent discussion, time will be EDT.) Pictures of the tornado's evolution are presented on the following pages to establish the extent of the tornado on 15 June, while the details of meteorological events in the mesonetwork are in section 5.

We first noticed a substantial raining cloud line from north to west to south of Central Site at 1500. By 1515, a new line oriented north to south was developing east of Central Site, where the wind was from the west. The tornado was first sighted at 1530 to the northeast in this new cloud line. One minute later we began photography and written observations. Figures 3 through 7 show every picture taken of the tornado from Central Site. Upper left figure 3 shows the first photo at 1531:15, toward the northeast, of a somewhat tilted funnel extending from cloud base to the surface, with rain behind it and to the north (left). Little change is evident ½ minute later. The lower pictures indicate some decrease in the intensity and tilt of the condensation funnel, while the rain and double cloud base have intensified. Upper left figure 4 indicates the turbulent clouds and some weak mammatus close to Central Site toward the northeast.

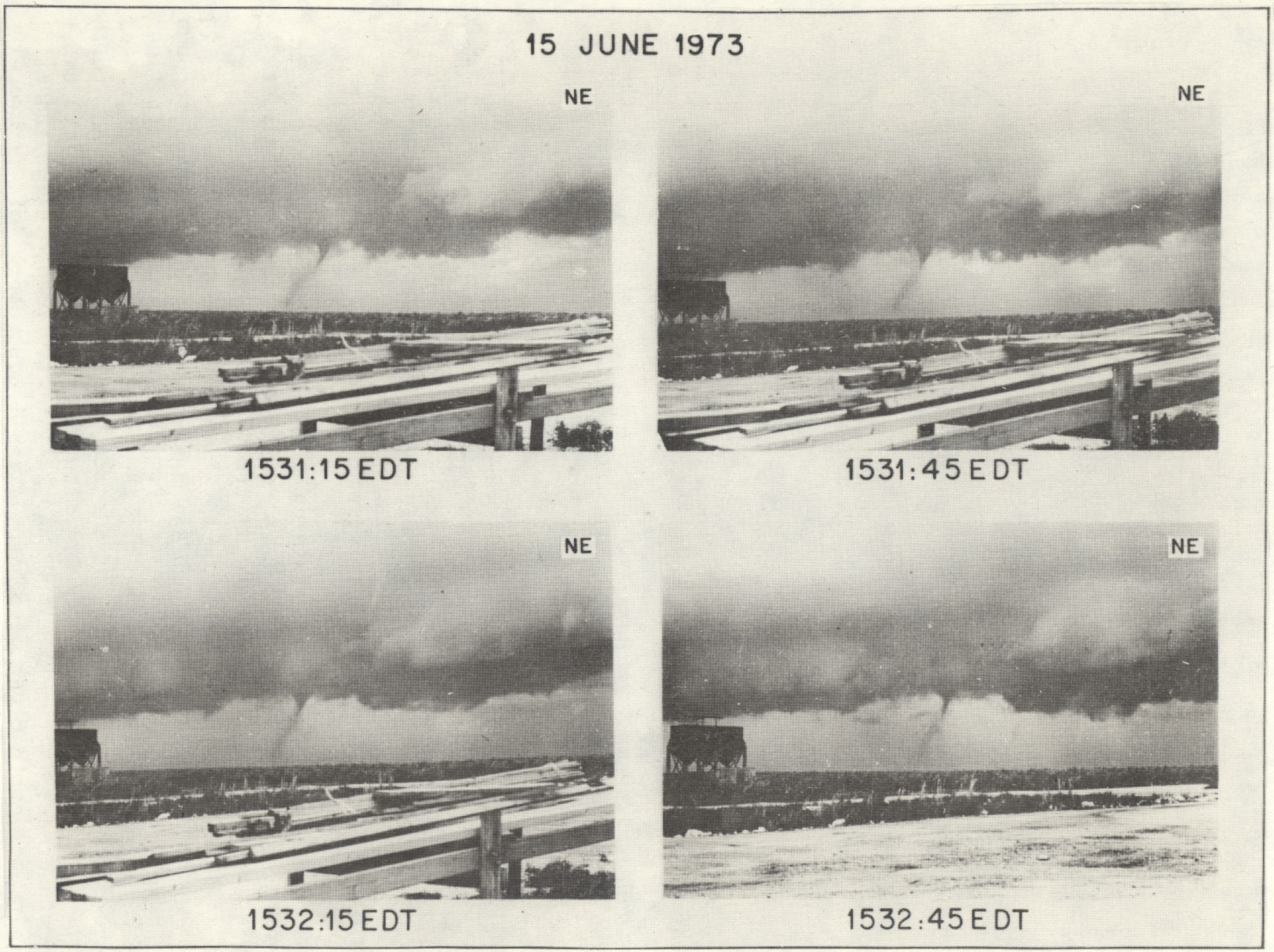

Figure 3. Views from Central Site of the 15 June tornado and attendant clouds in the FACE mesonetwork. Direction of each picture is shown in the upper right corner and time is below.

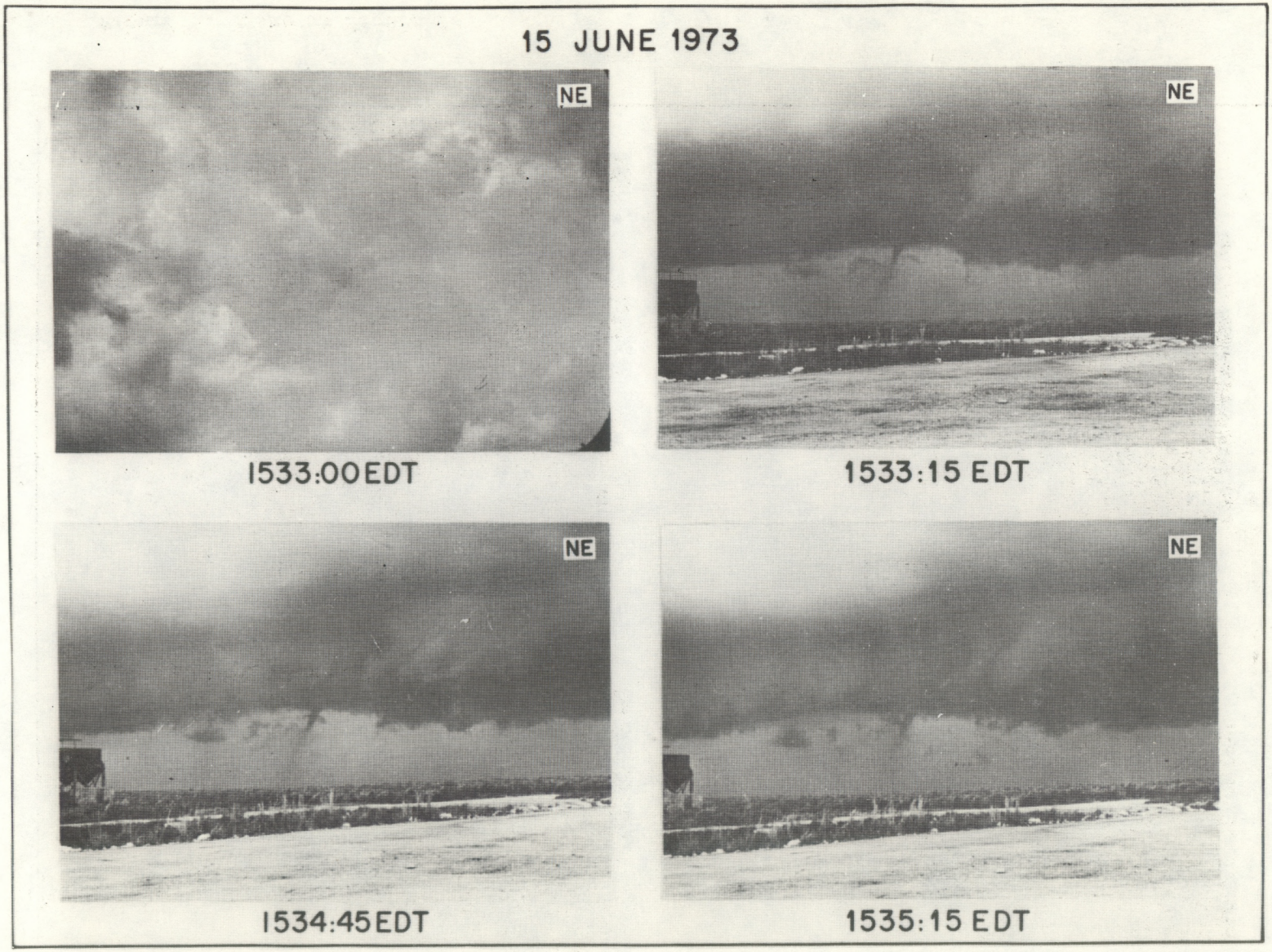

Figure 4. Same as figure 3.

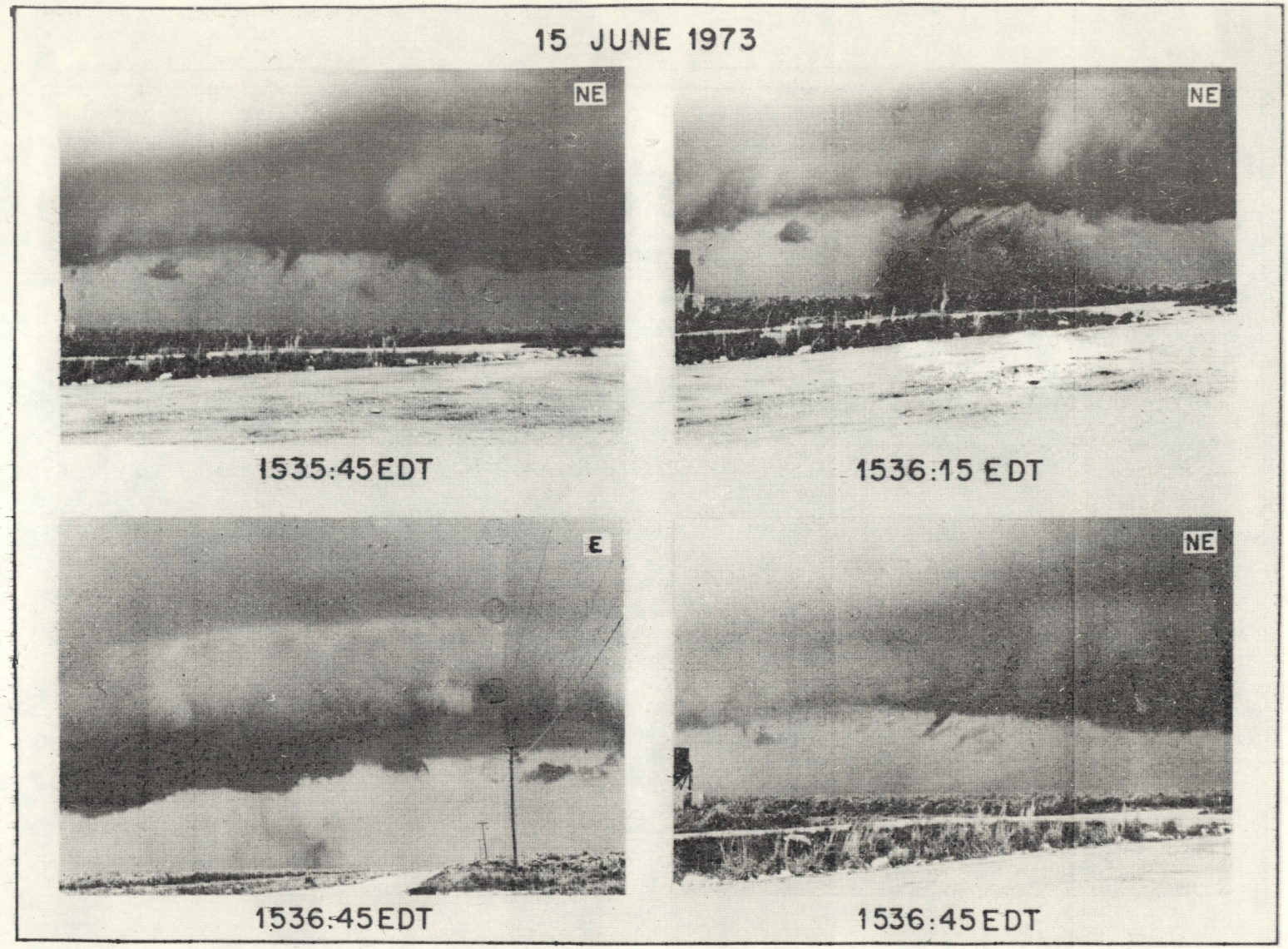

Figure 5. Same as figure 3.

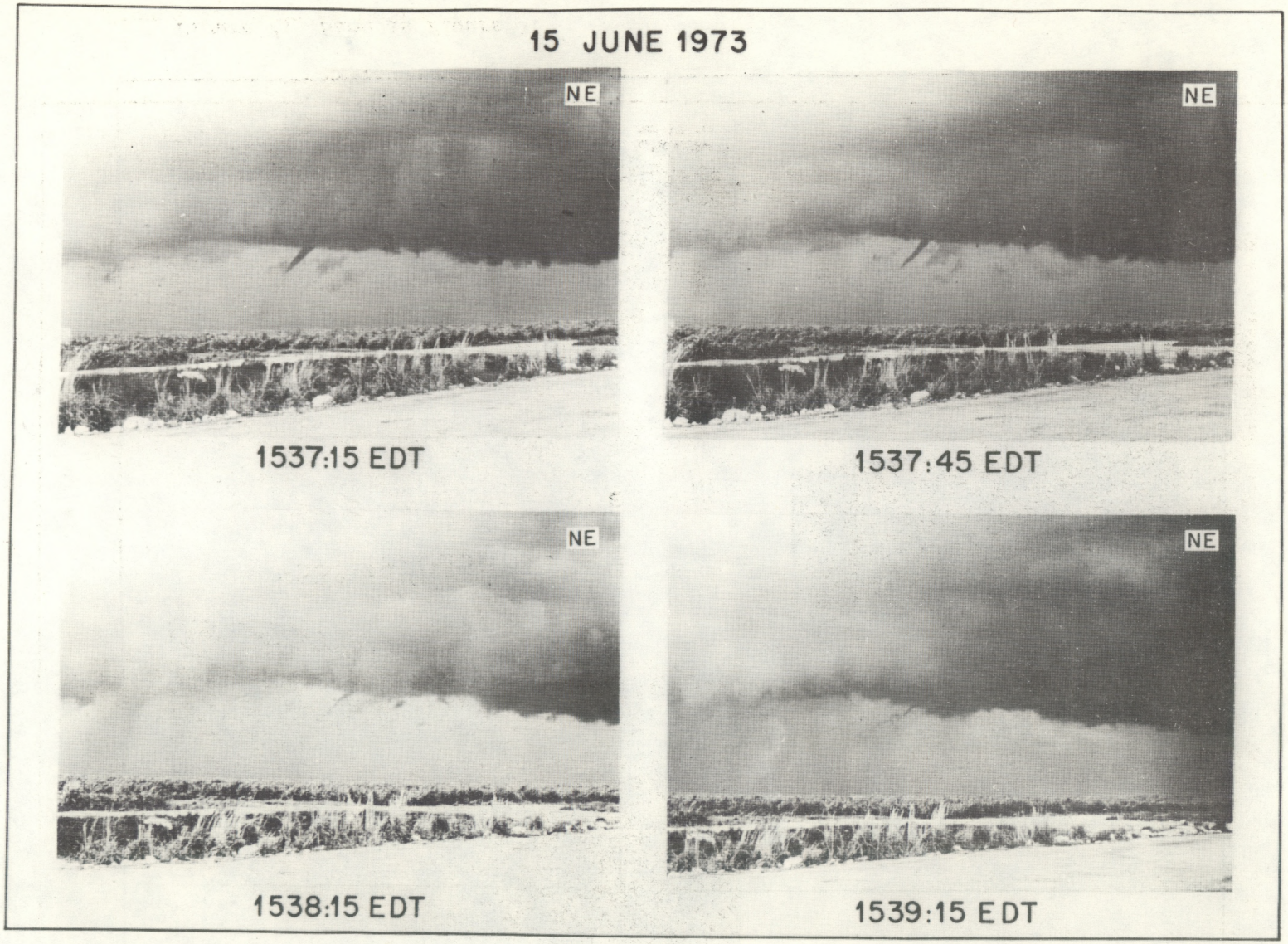

Figure 6. Same as figure 3.

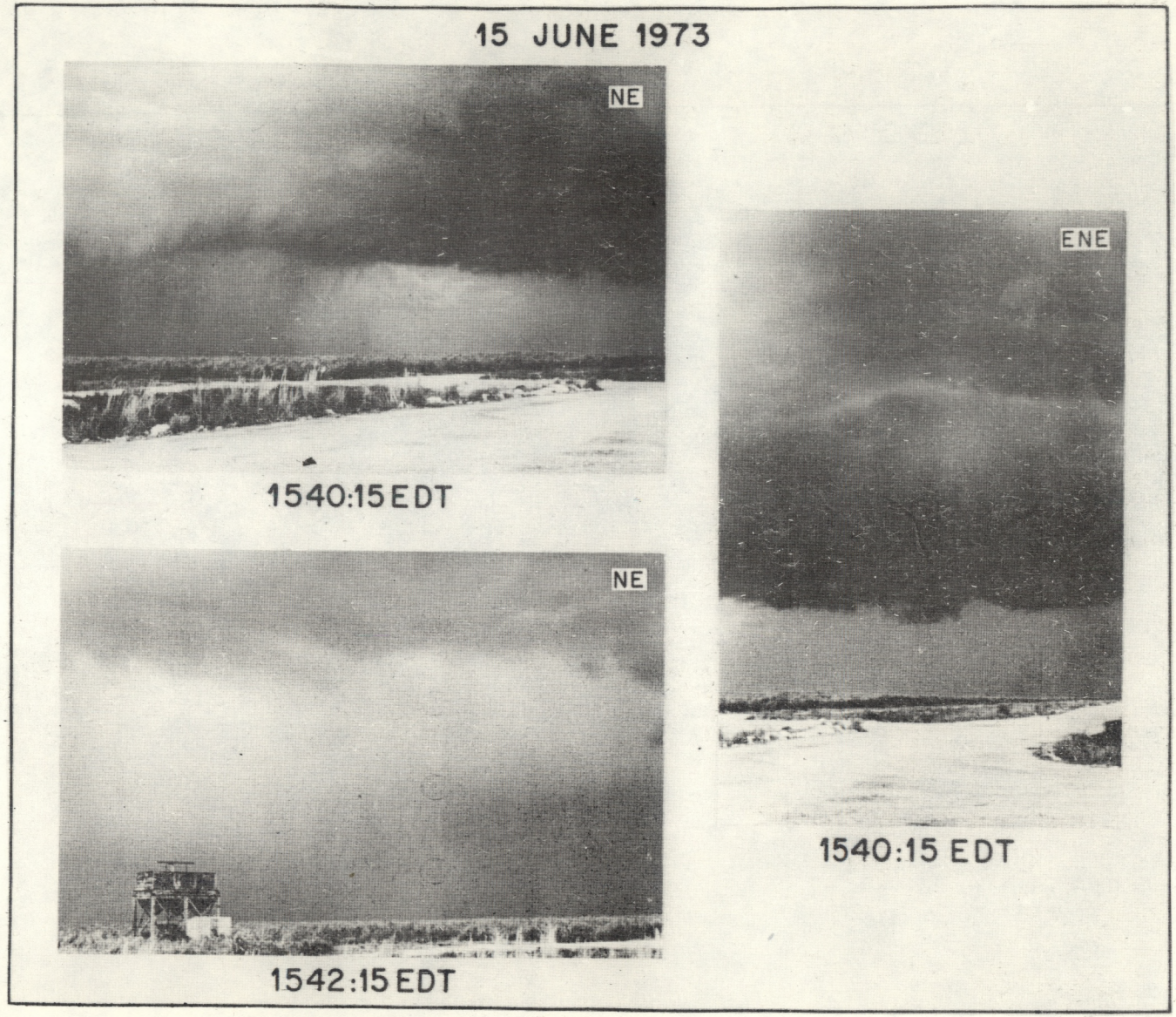

Figure 7. Same as figure 3.

over the next 2 minutes. The lower part of the funnel is not apparent, as it was before; however the original slide suggests a continuing connection to the surface. Rain in the background appears heavier than before. The lowest cloud base has a bulge toward the west that could represent a stronger rain shower behind the funnel than in other places on the parent cloud line. Upper figure 5 shows two more views of the funnel (now visible only near the cloud base) which, combined with a rather clear surface debris pattern, indicates a full extension from cloud to ground that in some earlier pictures was not visible. The 1535 view can be considered the middle of the tornado's life cycle. The picture at 1536:45 looks east toward an arcus cloud and double cloud base with smoke being raised at the surface. Rain is falling in the background. By 1537:15, in upper left figure 6, the tornado is beginning to narrow and tilt more strongly. Also at this time, the first rain is beginning to fall from the tornado's parent cloud line in a shower north of the vortex; previous rain had been behind the tornado (to the east). The tornado continues to dissipate after this time until at 1540:15, in upper left figure 7, the funnel is gone and rain is falling where the tornado had been. Less rain is falling from the cloud line south of the funnel location from 1539:15 to 1540:15, while a heavy cloud base and smoke continue further south in the line (right fig. 7). Two minutes later, at 1542:15 in lower figure 7, the former tornado position is the site of an intense rain shaft that was observed at the time to have a green hue, a frequent indicator of very heavy rain in Florida.

Photogrammetric analysis of the tornado was made with a method given by McNeil (1954). The technique requires knowledge of the camera and lens size, a visible horizon, and knowledge of distance to the measured feature. Results are shown in two ways. Table 2 lists the funnel length and width, and the cloud base height from each picture. Figure 8 shows these sizes, along with the shape of the visible features, on a time scale. The height scale of figure 8 also applies horizontally.

Table 2. Sizes of principal visible features of the 15 June 1973 tornado based upon photogrammetric analysis of pictures in figures 3 to 7

Time (EDT)	Cloud base height	Funnel length	Funnel width
1531:15	535 m	177 m	75 m
1531:45	514 m	147 m	128 m
1532:15	568 m	162 m	107 m
1532:45	557 m	151 m	53 m
1533:15	589 m	161 m	64 m
1534:45	589 m	161 m	75 m
1535:15	600 m	161 m	75 m
1535:45	589 m	167 m	96 m
1536:15	600 m	183 m	96 m
1536:45	622 m	183 m	118 m
1537:15	654 m	215 m	90 m
1537:45	654 m	220 m	96 m
1538:15	665 m	216 m	53 m
1539:15	686 m	107 m	21 m

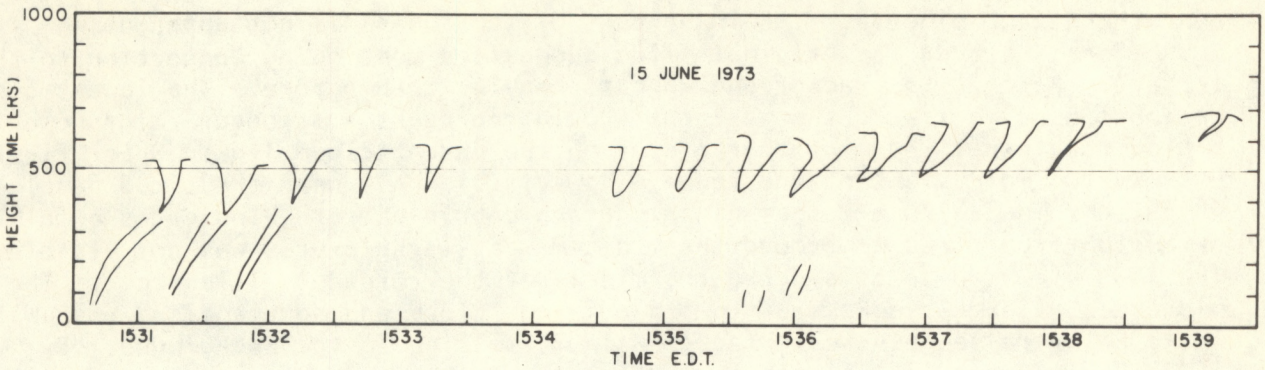

Figure 8. Time history of the size and shape of the condensation funnel shown in figures 3 through 7. The height scale also applies in the horizontal. The center of the funnel's intersection with cloud base is alined above the picture time. Values were determined by photogrammetric techniques described in text, and are listed in table 2.

Two significant features of the 15 June tornado are the narrowing of the funnel and the rise in cloud base as the tornado dissipates. The cloud base height rise may not be real, and could have been caused instead by the approach of the funnel to Central Site; the pictures support this view to some extent. However, this factor could not be included in calculations for lack of an objective way to determine it. A critical assumption in the calculations, then, is that distance from the camera at Central Site to the tornado was 6120 m. This distance is based upon the following: (a) figures 3 to 7 always show rain from a cloud line behind the tornado until it dissipates, and (b) the analyses of surface rain gage and radar data in section 5 help locate this cloud line. Based on the scale of features in these analyses, the distance estimate is probably accurate within 15%. The azimuth to the funnel was found by survey of the ground features in the pictures. The range of azimuths to the funnel is 050° to 054°, as shown in figure 2. Therefore, the tornado was probably within the area covered by the triangle as shown in figure 2 and in subsequent diagrams. The rotation of the funnel is thought to be cyclonic, based on analysis of the few scud clouds seen in the pictures.

Subsequent events indicated by our notes included little rain falling from the old cloud to the west at 1545, while the new cloud at the tornado's position continued to intensify. Light rain began at Central Site at 1600 and continued for several hours from a large, stratified anvil system.

3. SYNOPTIC SCALE

Conditions on the synoptic scale are far from the typical mid-latitude tornado environment. On 15 June there are light winds, no shear in the vertical, neutral stability, very weak trough conditions aloft, and no overall cloud motion in the tornado area. This contrasts with the high shear, rapid cloud velocity, unstable squall line environment of so many other tornadoes.

The surface maps for the region surrounding Florida on 15 June are shown in figure 9. At both map times there is essentially no pressure gradient over Florida. The tropical easterlies begin south of Florida, while a weak front is located over the Atlantic Ocean near 30° N. The frontal position is based on satellite imagery (to be shown later) and additional surface data not presented in figure 9; these data combine to indicate very little support for extension of the front to South Carolina or Florida. The point is significant because Florida cannot be said to be under frontal influences. A weak trough is evident on the 2000 surface chart, but this is a typical afternoon feature induced by heating over Florida. Winds at the gradient level in the tropics, shown by the ATOLL (Analysis of the Tropical Oceanic Lower Layer) chart, are gathered routinely at NHC (National Hurricane Center) of NOAA in Coral Gables, and analyzed objectively by NMC (National Meteorological Center) of NOAA in Suitland, Maryland. This and other NHC products are discussed by Wise and Simpson (1971). The ATOLL chart includes 2000-ft. land station winds (plotted here), low-level satellite winds, surface ship winds, and aircraft winds below 5000 ft. Zero winds are indicated by a plus. Evidence of a weak ridge over south Florida is seen on the morning ATOLL charts, separating westerlies in the Tampa area northward from easterlies in the Miami area southward. At 2000, light northerly flow of a few m s^{-1} is found in the study area due to an anticyclonic circulation in the eastern Gulf of Mexico.

Higher level charts are shown in figure 10. At 500 mb there is such a lack of gradient in heights and temperatures that no analysis was attempted, especially with the lack of data east of 80° W. Some evidence of a trough at 500 mb is seen, particularly at 2000 EDT. The 200-mb analyses in figure 10 are again a combination of observed 200-mb winds and satellite winds collected by NHC and analyzed objectively at NMC. The cyclonic circulation west of Cuba at 200 mb may also be present at 500 mb, but is not easily detected there. Fairly conservative features on both maps include a col in the Bahamas and easterly flow over peninsular Florida.

Mean layer charts are also produced daily at NHC to delineate broad motion systems in the tropics. The charts are based only on fixed stations, with a few bogus point values introduced by the NHC analyst. The lower troposphere maps (1000 to 600 mb) in figure 11 show light winds which reverse from morning westerlies to evening easterlies over south Florida. Winds are so light that Miami and Key West mean winds oppose each other and the analysis could not draw for both. The upper troposphere mean charts in figure 11 show east to northeast flow over south Florida in the morning changing to southerly in the afternoon. The low, or trough, over western Cuba is consistent with lows on the 200-mb maps in the same place.

The deep layer mean charts in figure 12 were also made by NHC, and apply to the entire layer from 1000 to 200 mb. They show northerly flow over south Florida in the morning and easterly in the evening, but flow is under 4 m s^{-1} at both times. Shear between the upper and lower tropospheric means is shown in lower figure 12, and is so weak over south Florida that direction patterns change

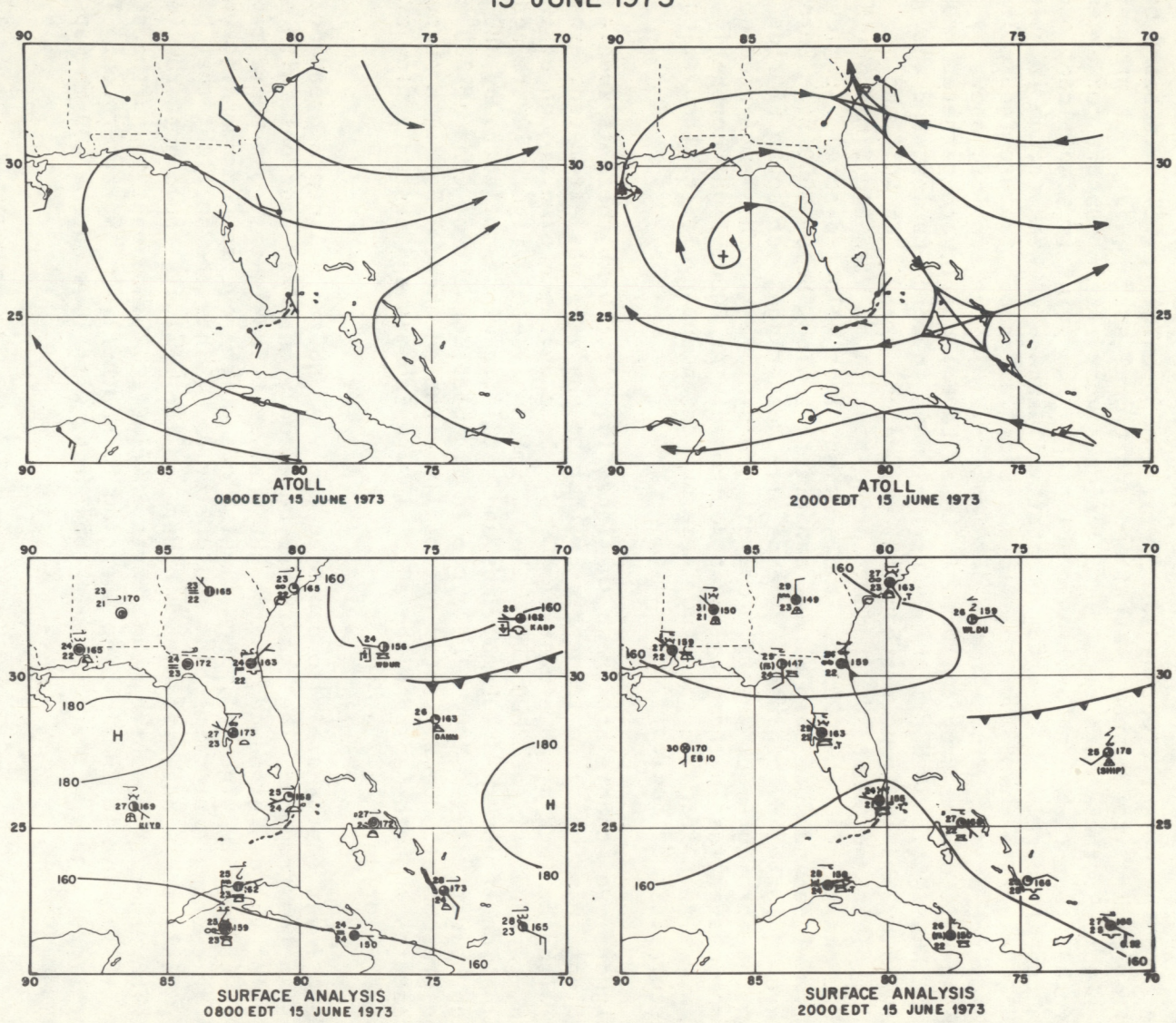

Figure 9. Surface weather and low-level wind charts on 15 June at 0800 and 2000 EDT. Full wind barb is 5 m s^{-1}. Zero winds indicated by a plus sign.

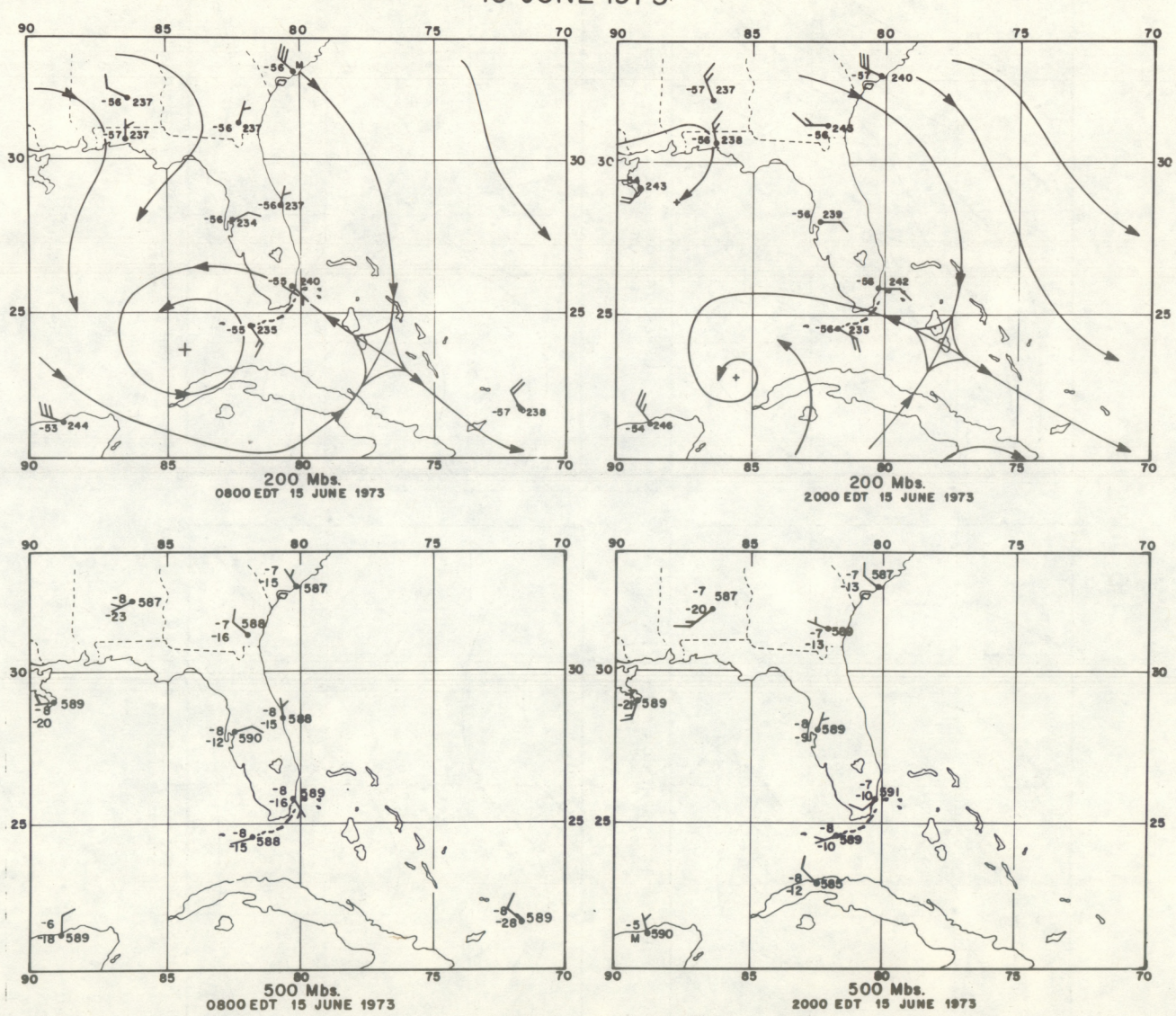

Figure 10. Maps of 500- and 200- mb levels on 15 June at 0800 and 2000 EDT. Zero winds indicated by a plus sign. Full wind barb is 5 m s^{-1}.

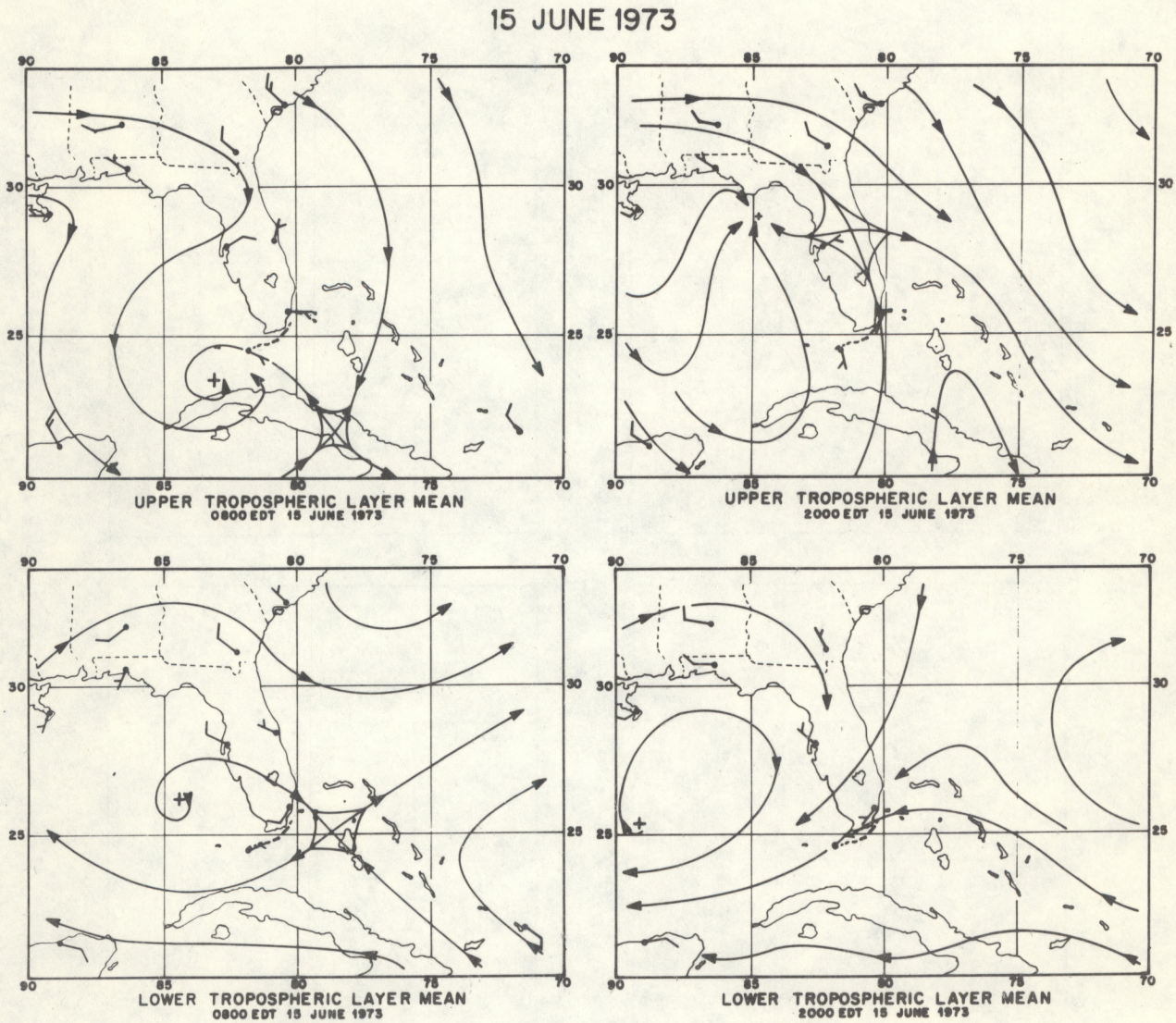

Figure 11. Mean layer charts on 15 June 1973 at 0800 and 2000 EDT. The lower mean applies to the layer from 1000 to 600 mb, while the upper is from 600 to 200 mb. Zero winds indicated by a plus sign. Full wind barb is 5 m s^{-1}.

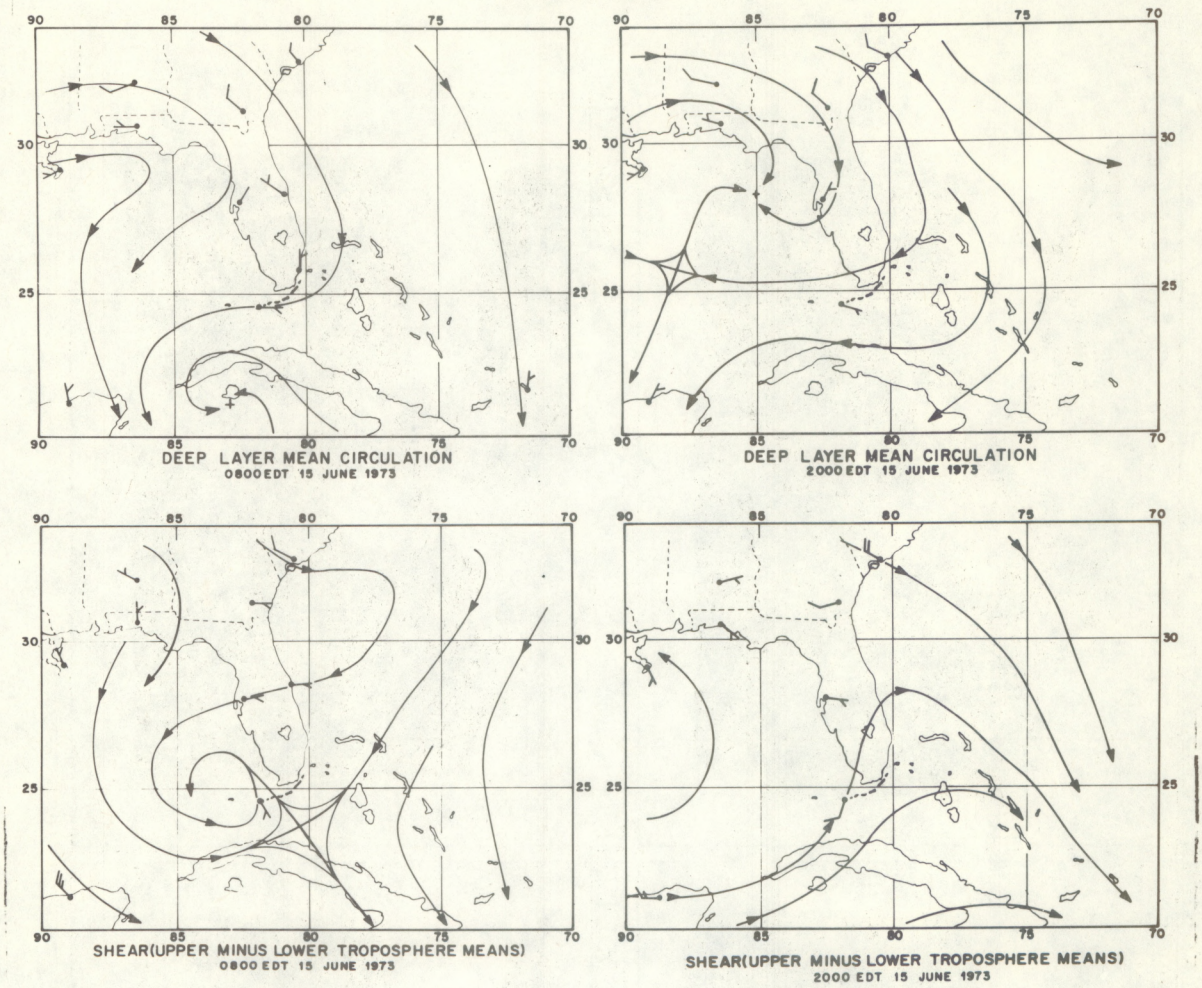

Figure 12. Deep layer mean circulation (upper panels) from 1000 to 200 mb on 15 June at 0800 and 2000 EDT. Shear charts (lower panels) are derived from the difference between the upper mean charts and the lower mean charts in figure 11. Zero winds indicated by a plus sign. Full wind barb is 5 m s^{-1}.

significantly during 15 June. The shear chart shows clearly that south Florida is in a light flow regime surrounded by steadier and stronger flow in all directions away from the state.

The ATS-3 satellite data on 15 June are shown in figures 13 and 14. Indicated times are for scan line passage over Florida. The last three panels vary in appearance because they were derived from a different recovery process than the first five panels. In relation to the synoptic scale features just shown, the satellite imagery at 0928 shows little cloudiness, except cold frontal clouds east of Florida. Later in the day, the 1643 data show cumulonimbus anvils being blown eastward over eastern Cuba and northwestward over western Cuba. This pattern fits the 200-mb charts of figure 10 quite well. But over Florida, where all maps showed weak winds, the clouds on satellite imagery have

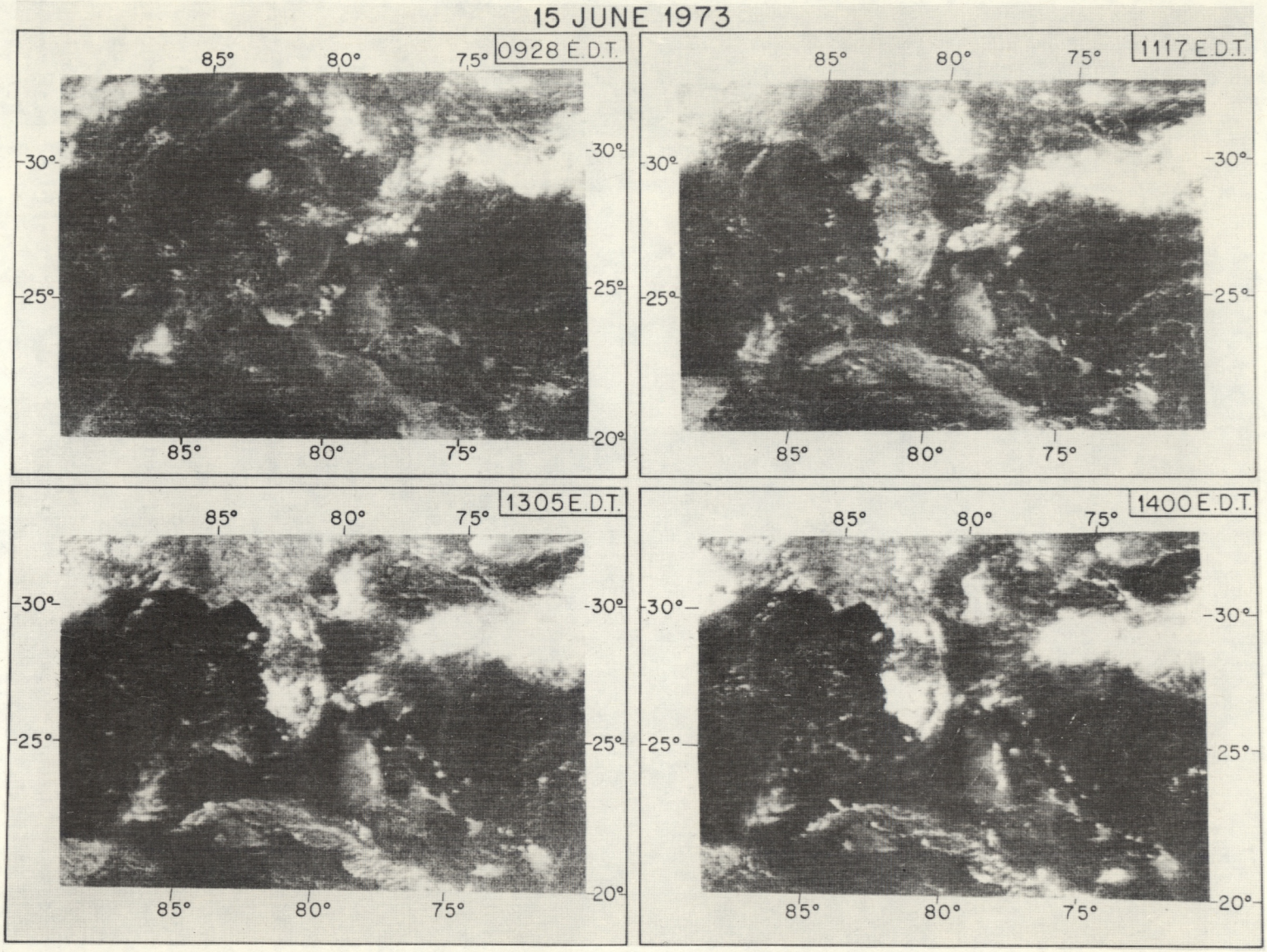

Figure 13. ATS-3 satellite imagery on 15 June. Times are for data collection over Florida. Correct grids are shown by tick marks on the borders.

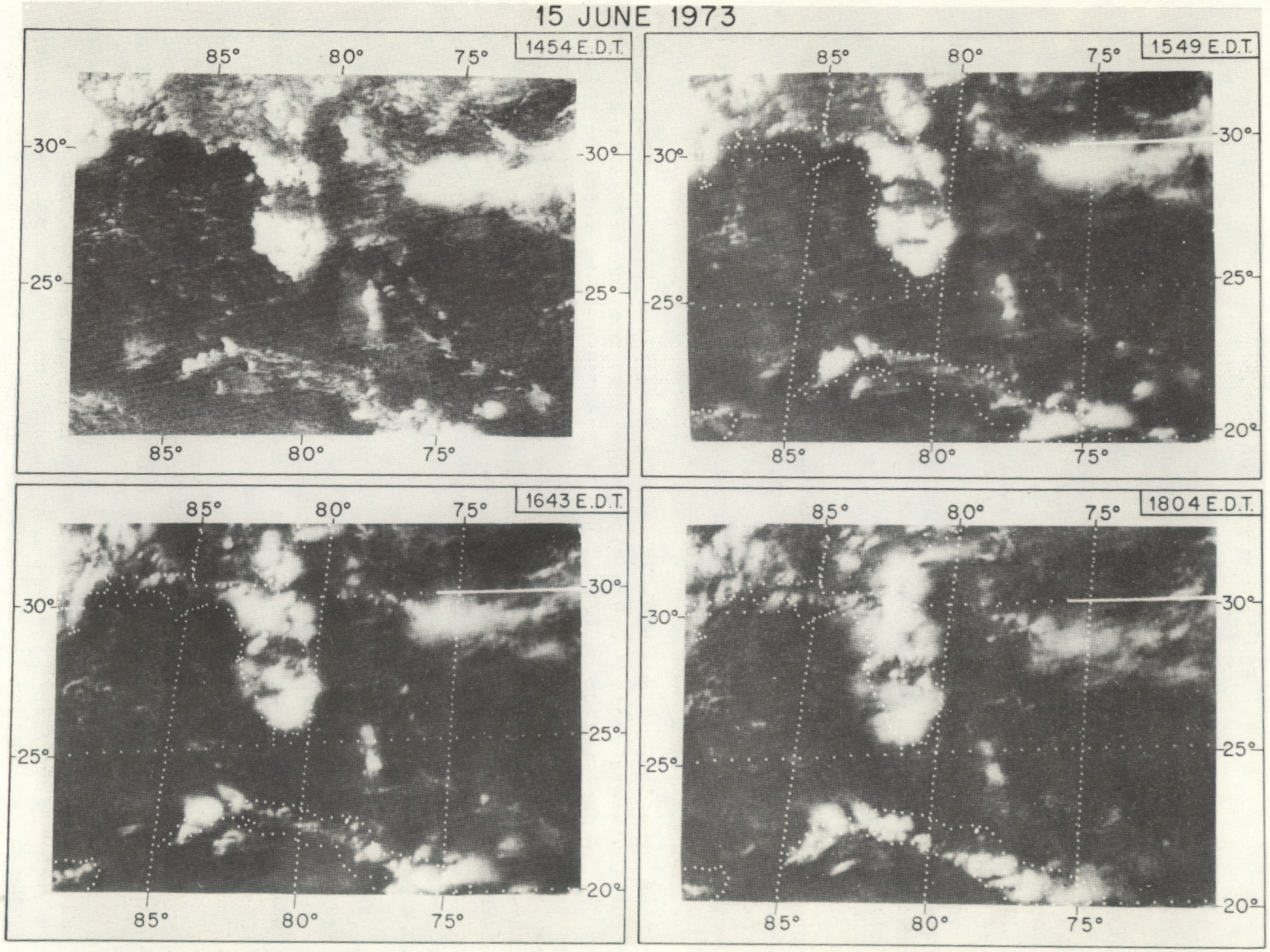

Figure 14. ATS-3 satellite imagery on 15 June. Times are for data collection over Florida. Correct grids are shown by tick marks on the borders.

moved little beyond the coastlines of the peninsula by day's end.

4. PENINSULAR FLORIDA SCALE

The satellite imagery of figures 13 and 14 can be used to show cloud development over Florida, as well as the synoptic-scale features just considered. At the start of the day, the 0928 satellite data show some clouds on the southwest Florida coast, which merge across the state by 1117. A small, but continuous, cloud line is evident at 1117 along the southeast coast. This is the sea breeze line studied observationally and theoretically by Pielke (1974). By 1400 there is a sea breeze line most of the way from Miami to Jacksonville along Florida's east coast, but it has remained near the coastline, consistent with a lack of significant wind flow. Clouds over southwest Florida are also organized, here in a larger mass. However, there is a distinct open area between the sea breeze and the western mass at 1400. At 1549, 9 minutes after tornado dissipation in the mesonetwork, a rather large and mostly continuous cloud mass exists over south Florida, and merges more completely by 1804.

Figures 15 through 24 show the evolution of the environment around the tornado in south Florida. These hourly maps provide information on the intermediate scales between the synoptic-scale patterns of the previous section and the mesonetwork scale of the next. Observed echo motion was "zero" or "little movement" at all times on 15 June.

At 0948, the 10-cm Miami WSR-57M radar showed (fig. 15) that showers were just off the southwest coast. These clouds are also seen on satellite at 0928 in figure 13. A maximum top height of 9.5 km was measured by radar in this line 8 minutes earlier. The heaviest rainfall is indicated by the black dot within the white area in one of the more northerly showers, corresponding to a rain rate of between 13.7 and 30.2 mm hr^{-1} (see fig. caption). Surface stations at 1000 in figure 15 show no wind pattern, except southeast winds in the Keys, a flow that continues most of the day. Temperature and pressure show little gradient, except interior stations are warmer. No clouds exceed the cumulus congestus stage.

By 1107 the first clouds have moved or re-formed inland from the southeast coast (fig. 16), and new echoes have formed near Lake Okeechobee. Maximum tops are 7.3 km along the southwest coast and 6.7 km east of the lake. Easterly winds have begun at some southeast coastal stations as the sea breeze establishes itself. Rain and towering cumuli are reported at Fort Myers near the radar echoes.

Two hours later at 1300 (fig. 17) the southeasterly flow has established itself at all east coast stations from West Palm Beach southward. Recall that satellite data indicated a nearly solid line there by 1305 in figure 13. However, the radar data at 1302 in figure 17 do not show an extensive north-south raining sea breeze, indicating that clouds in the line are not too deep. A major rain area has developed between Lake Okeechobee and the southwest coast, where Fort Myers is reporting a thunderstorm at 1300. The maximum echo top was 14.6 km 20 minutes earlier in the large storm just southeast of Fort Myers.

Figures 15 through 24

Extended caption for hourly map of peninsular Florida on 15 June 1973

Hourly map of peninsular Florida on 15 June. Surface synoptic data on right are from regular reporting stations plus special data sources in FACE. Full wind barb represents 5 m s^{-1}. Miami WSR-57M radar data are on left at the indicated time. Outer echo outline is at 0.25 mm hr^{-1} rainfall rate; next contour is 2.3 mm hr^{-1} and encloses a white area; next contour is 13.7 mm hr^{-1} and encloses a black area; next is 30.2 mm hr^{-1} and encloses a white area. A hatched area shows that precipitation was present, but intensity is unknown, either because the return is affected by anomalous propagation or is beyond the 125 n.mi. range within which echo intensities are recorded. The polygonal area south of Lake Okeechobee on the radar chart represents the mesonetwork of figures 1 and 2.

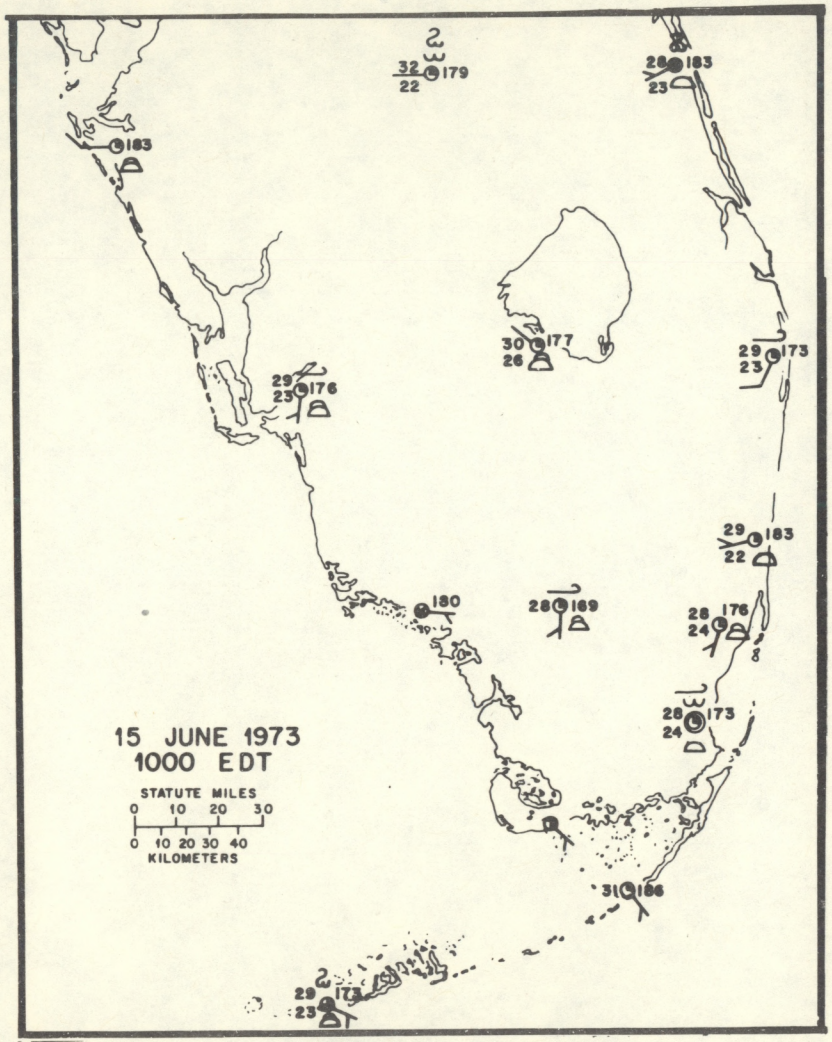

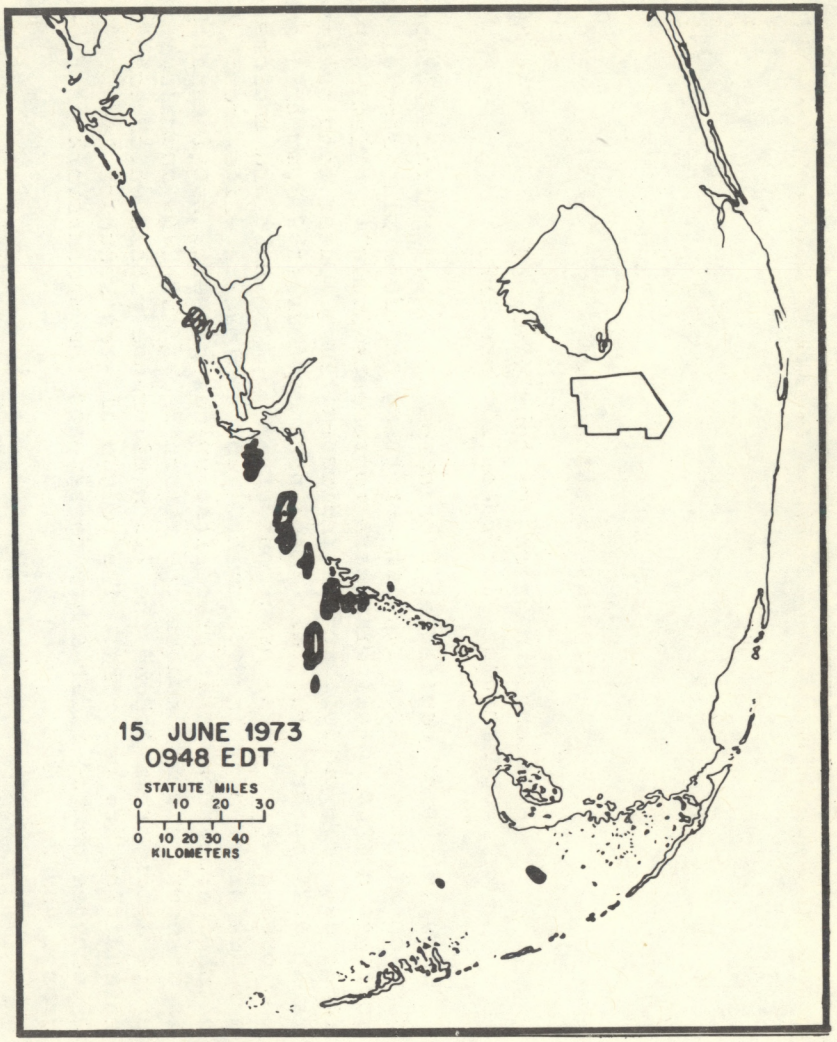

Figure 15. See extended caption, page 21.

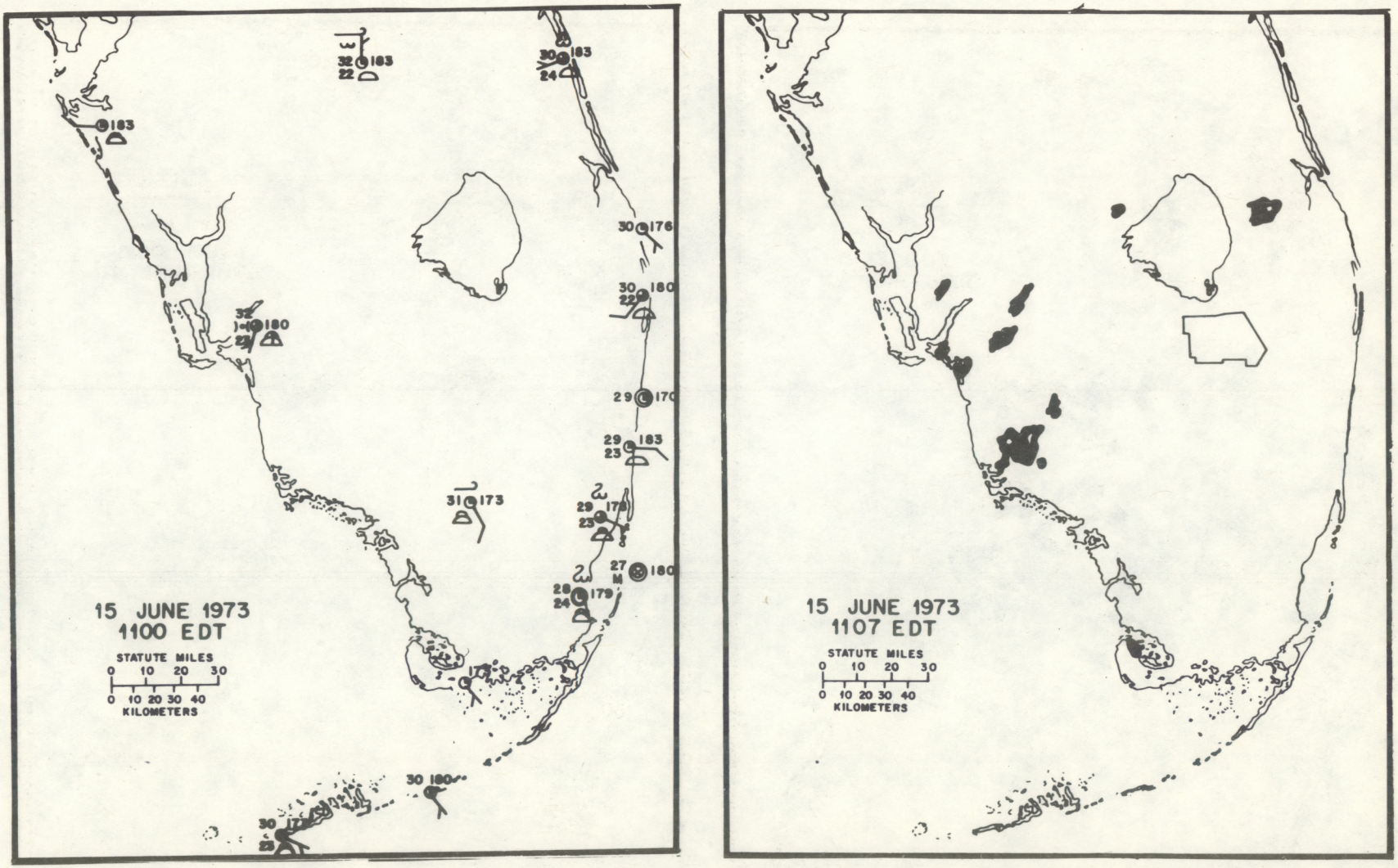

Figure 16. See extended caption, page 21.

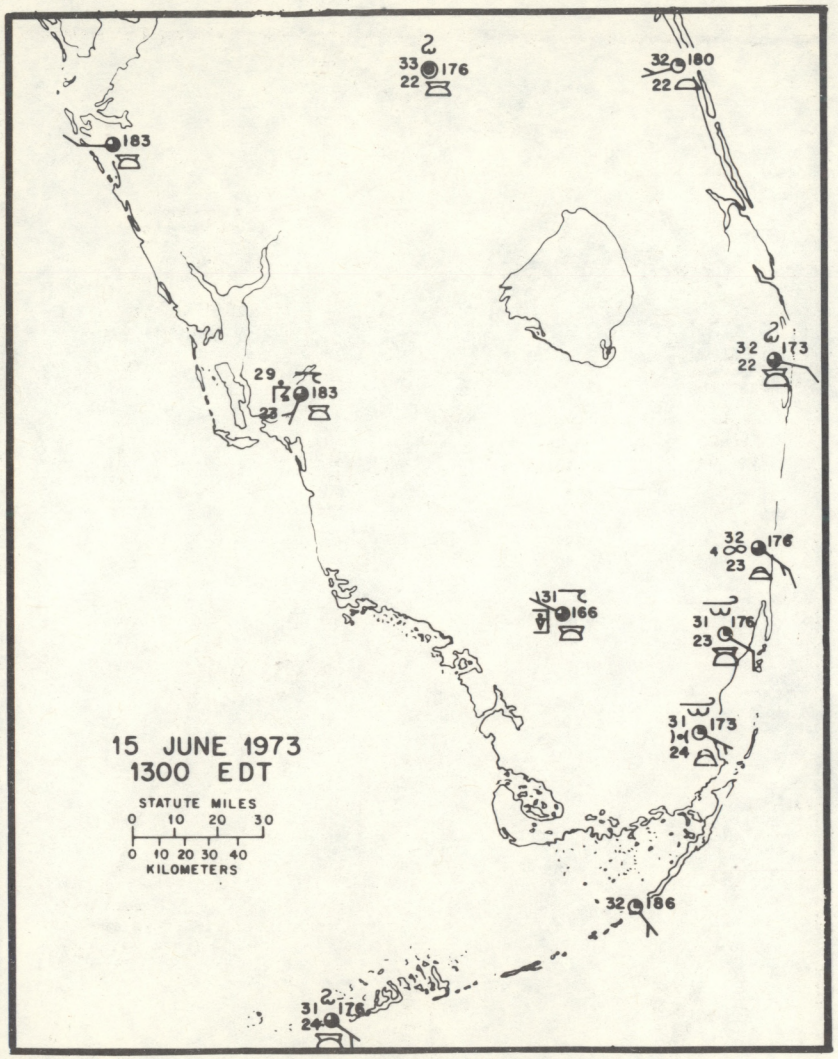

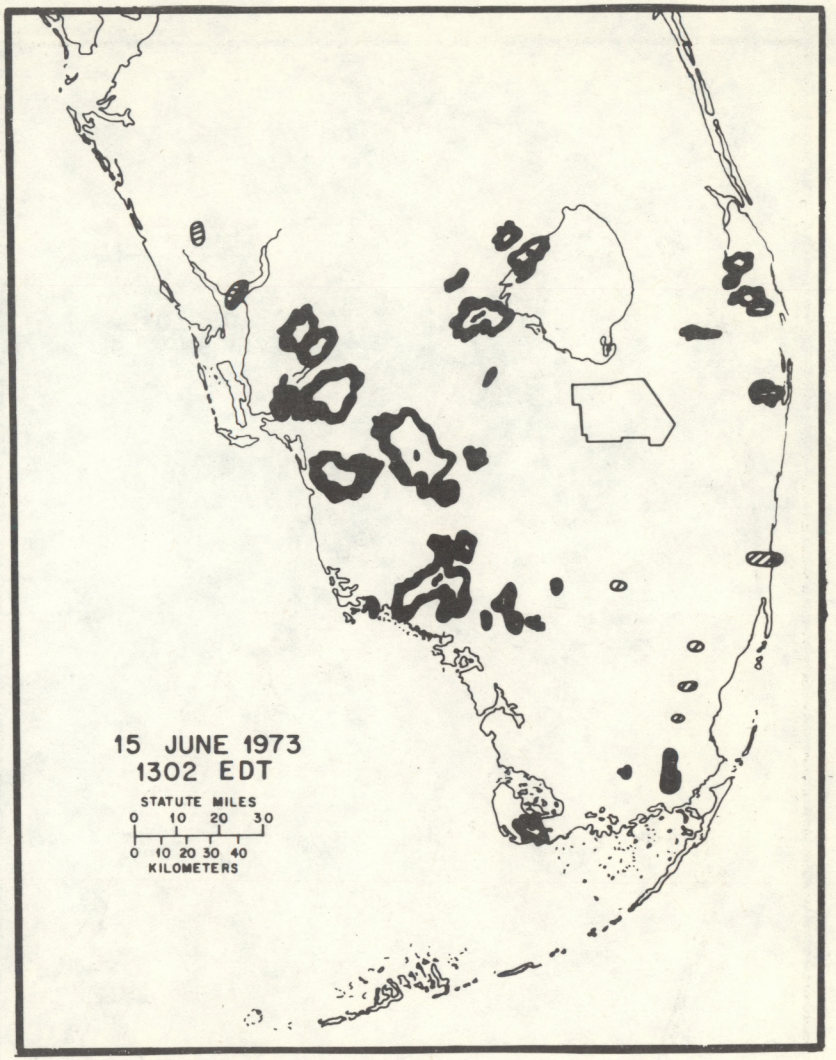

Figure 17. See extended caption, page 21.

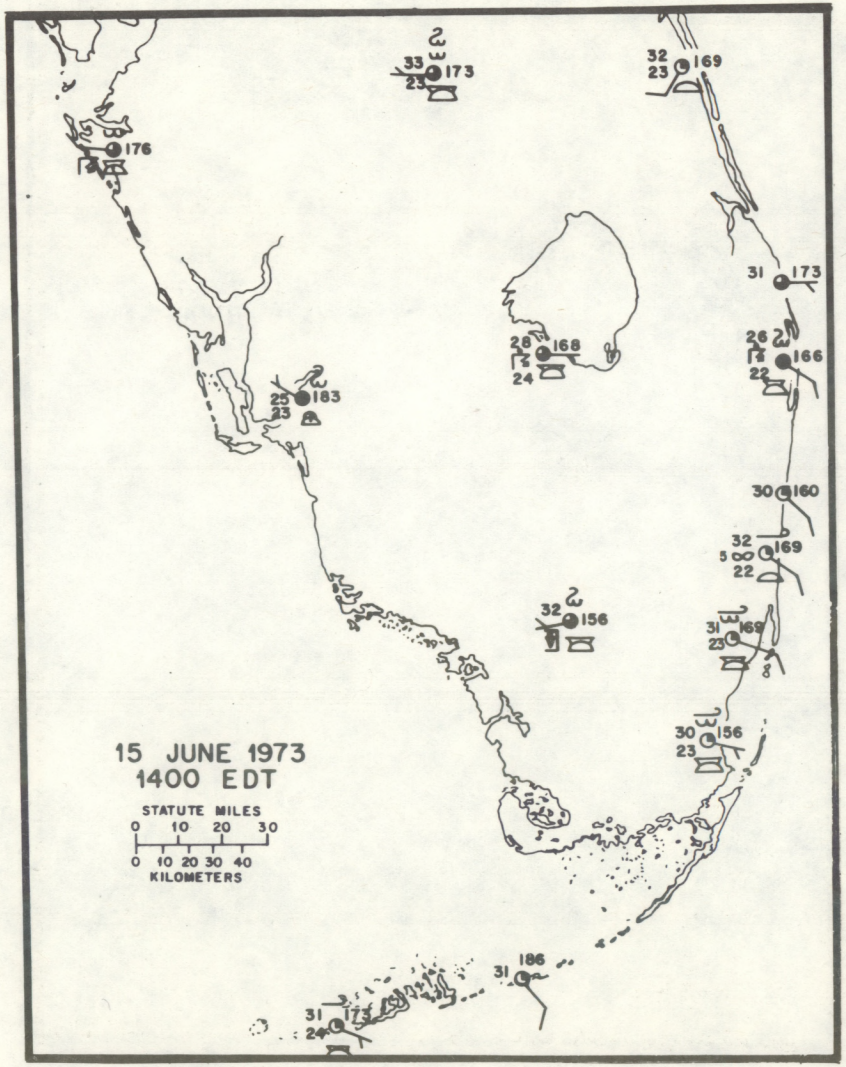

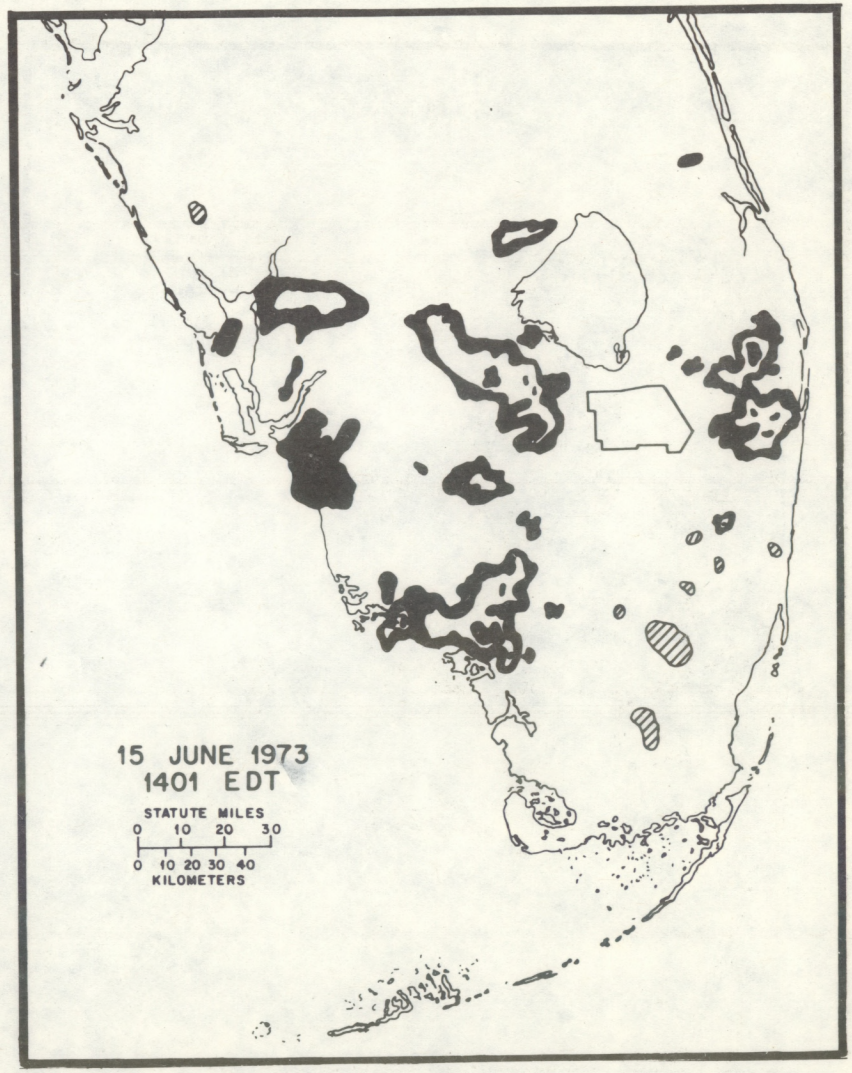

Figure 18. See extended caption, page 21.

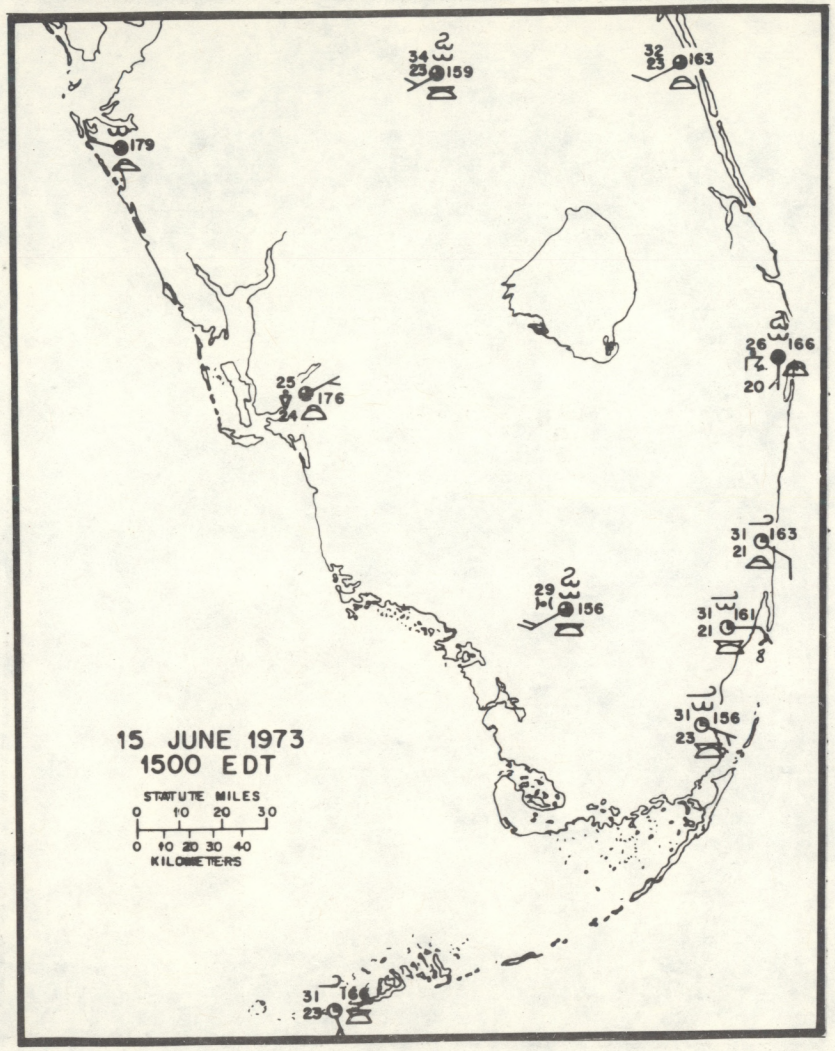

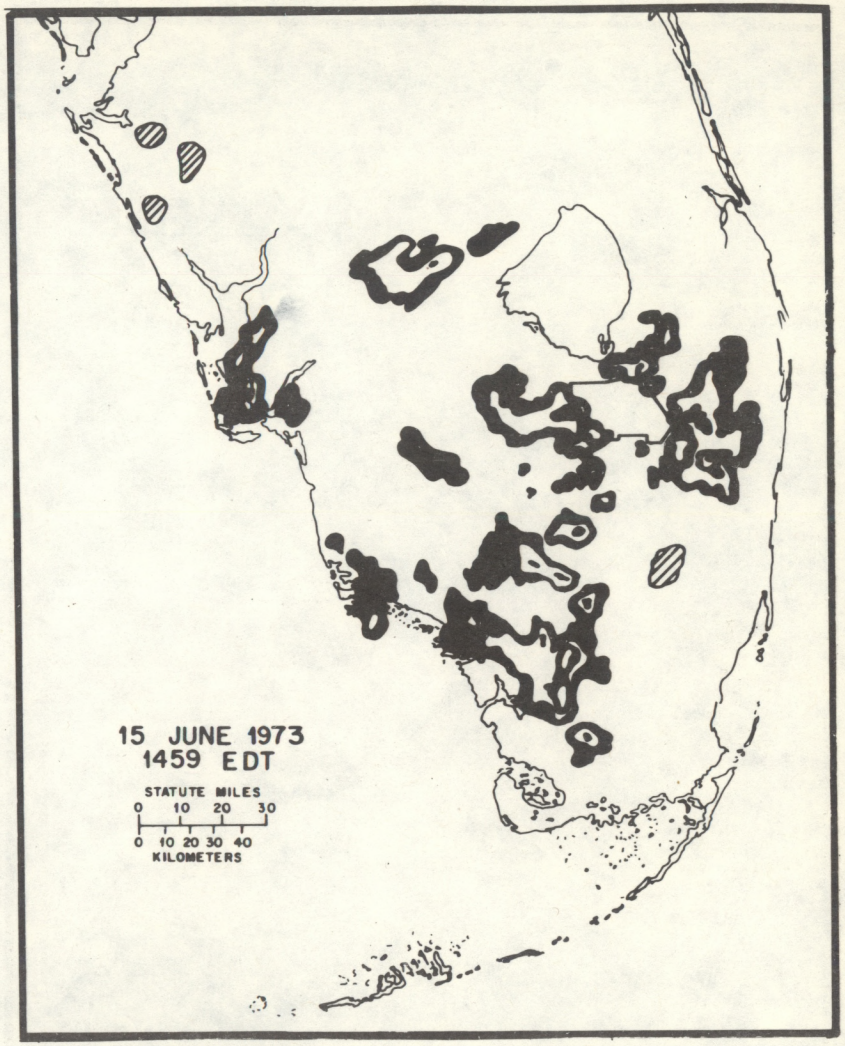

Figure 19. See extended caption, page 21.

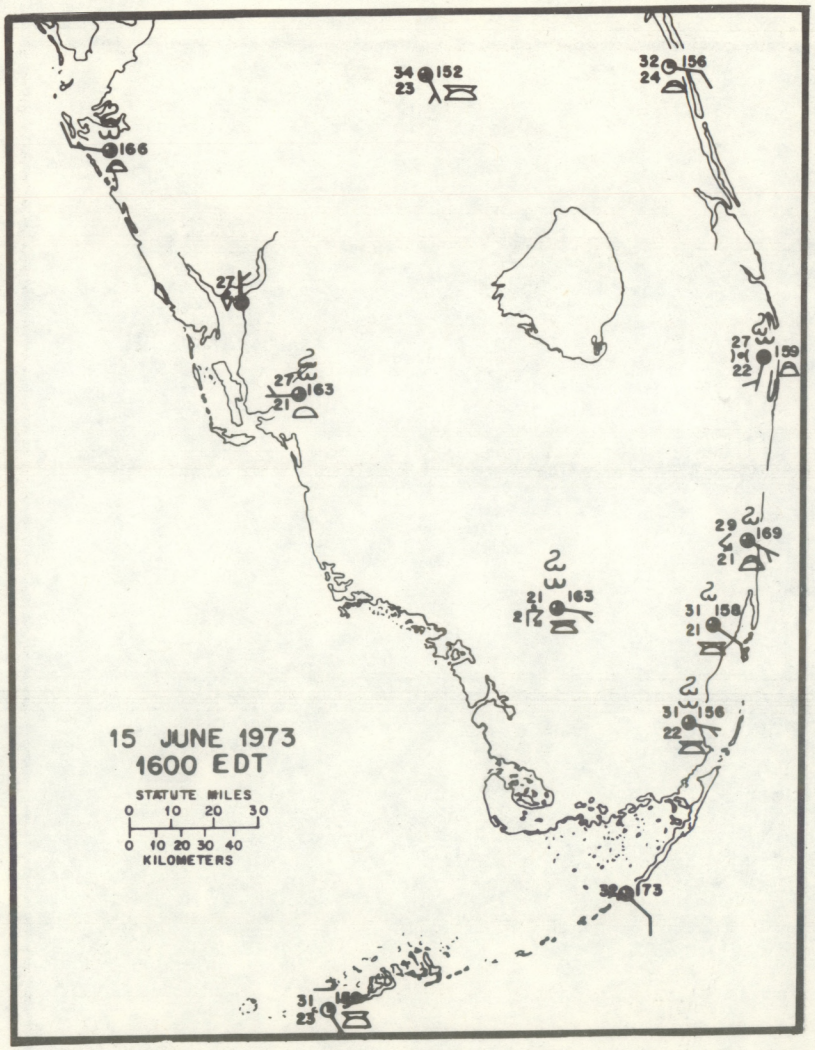

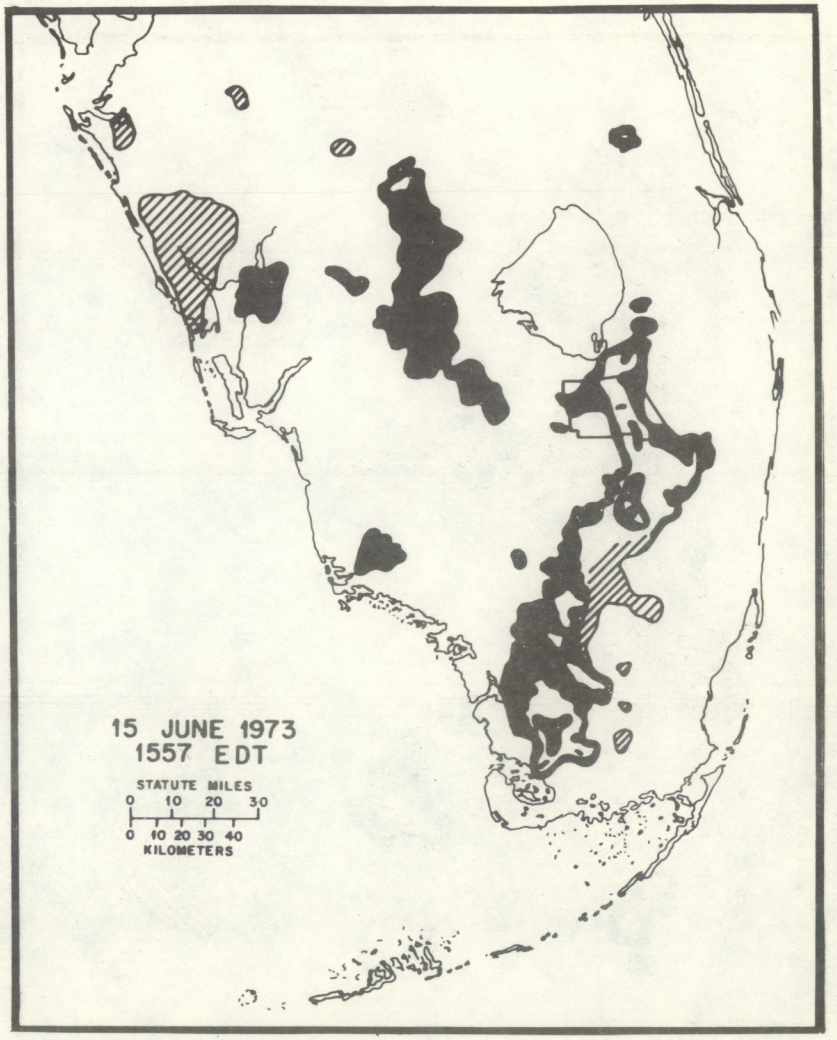

Figure 20. See extended caption, page 21.

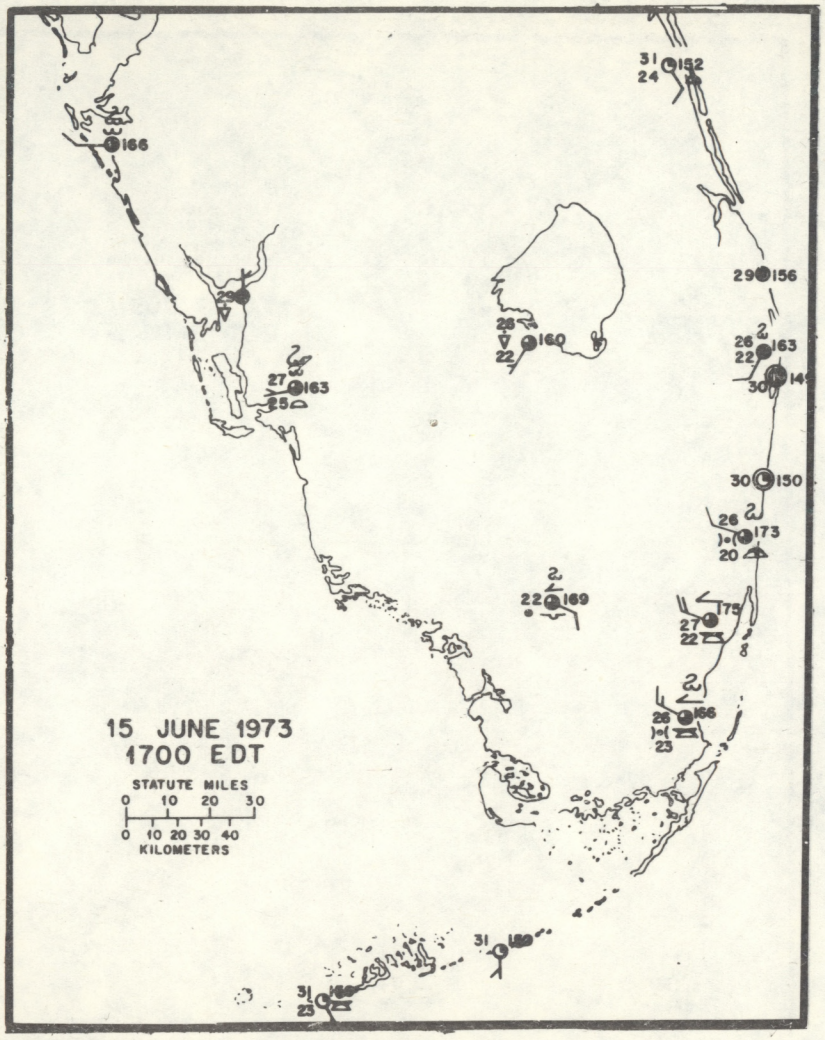

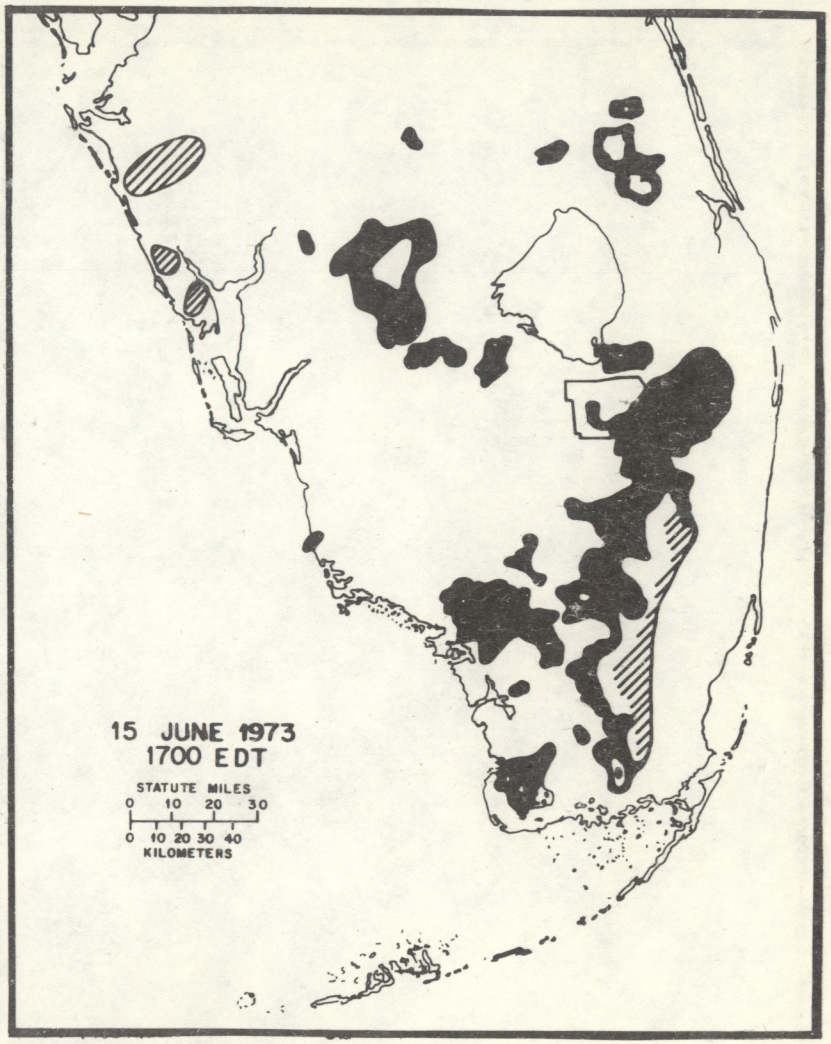

Figure 21. See extended caption, page 21.

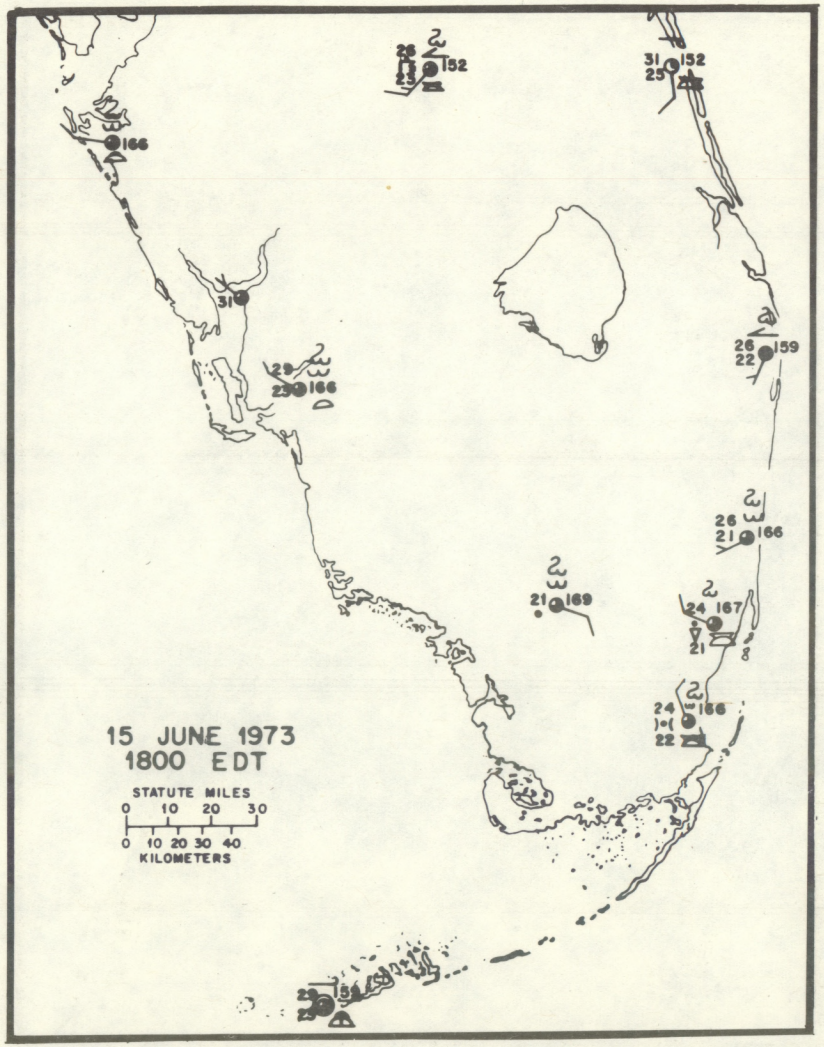

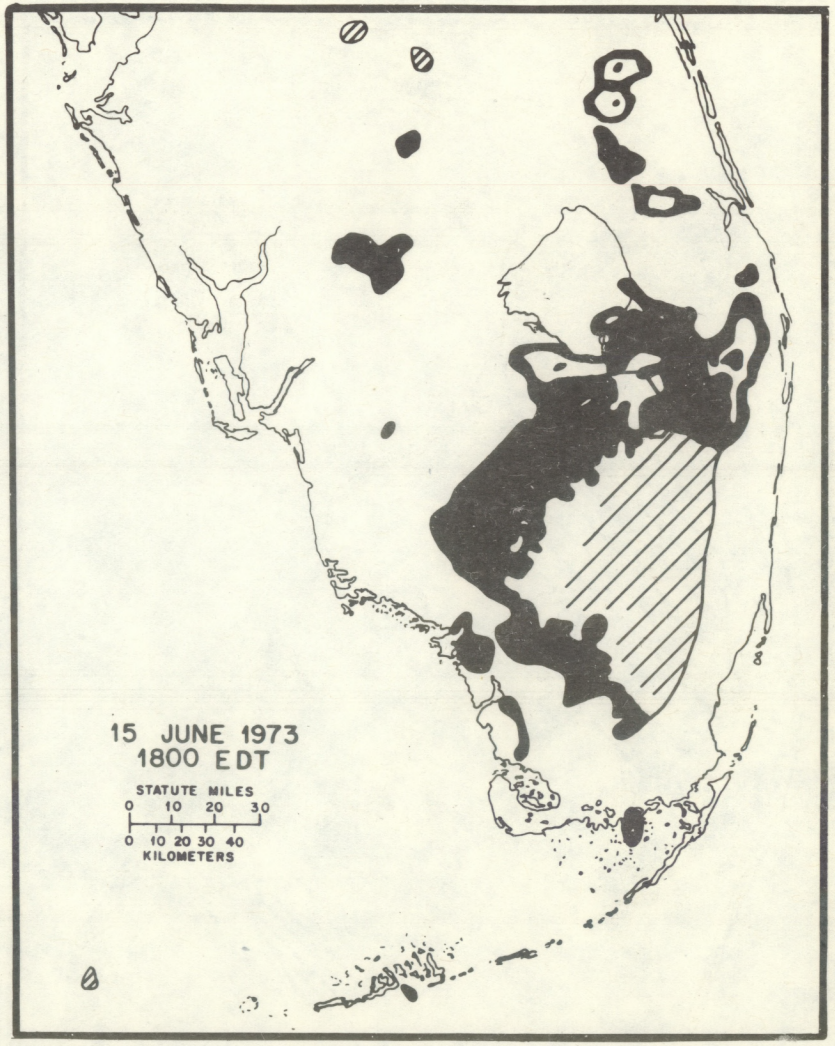

Figure 22. See extended caption, page 21.

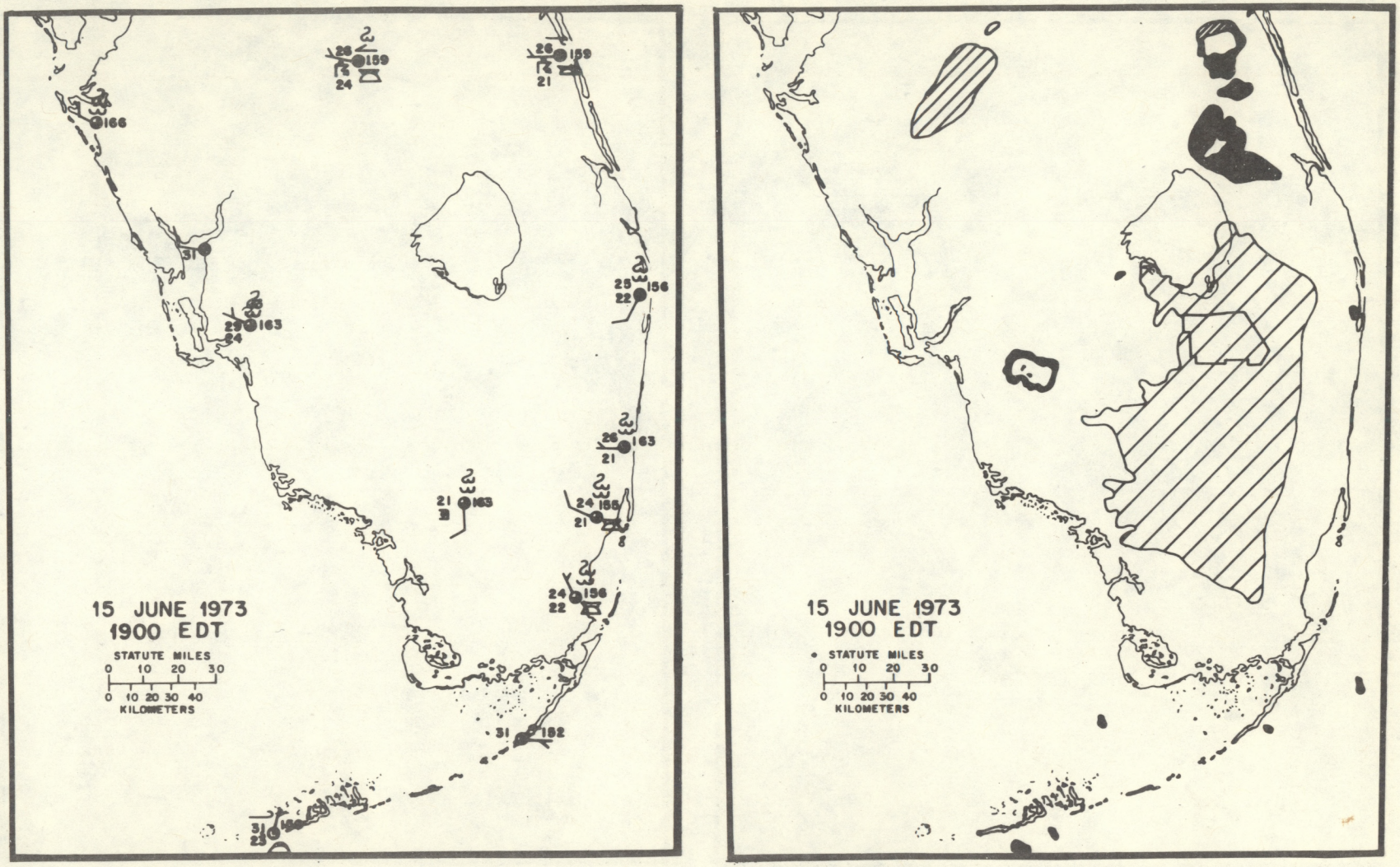

Figure 23. See extended caption, page 21.

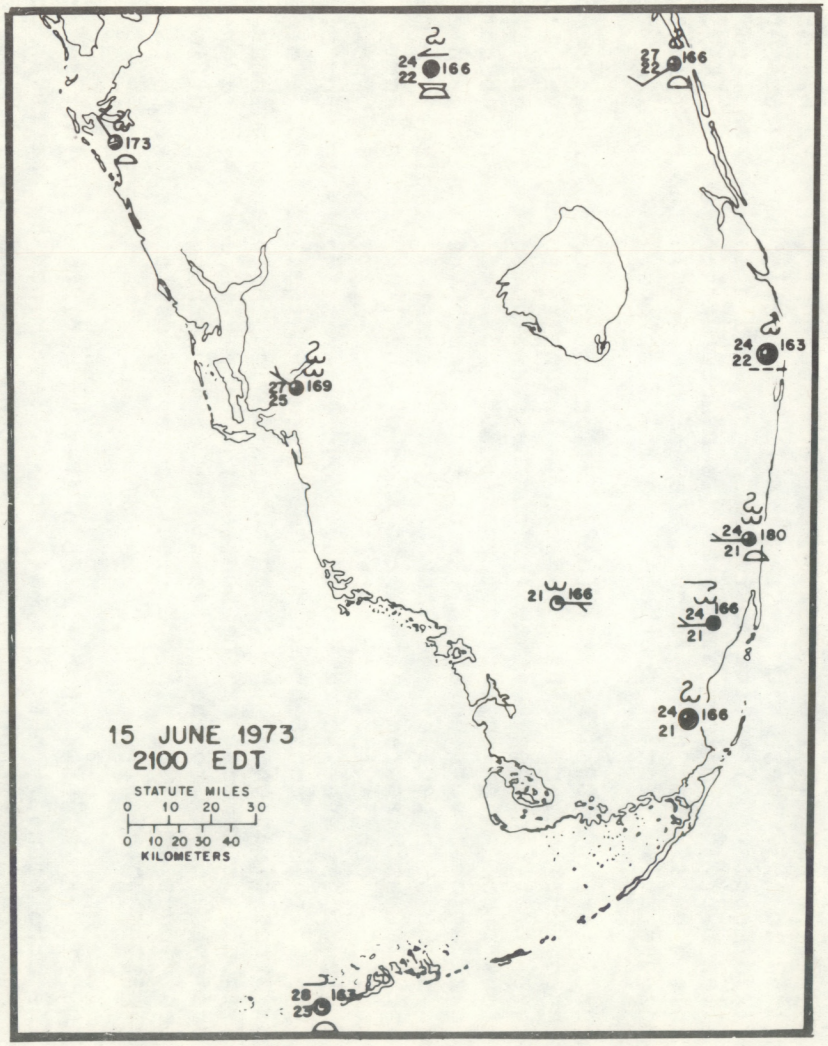

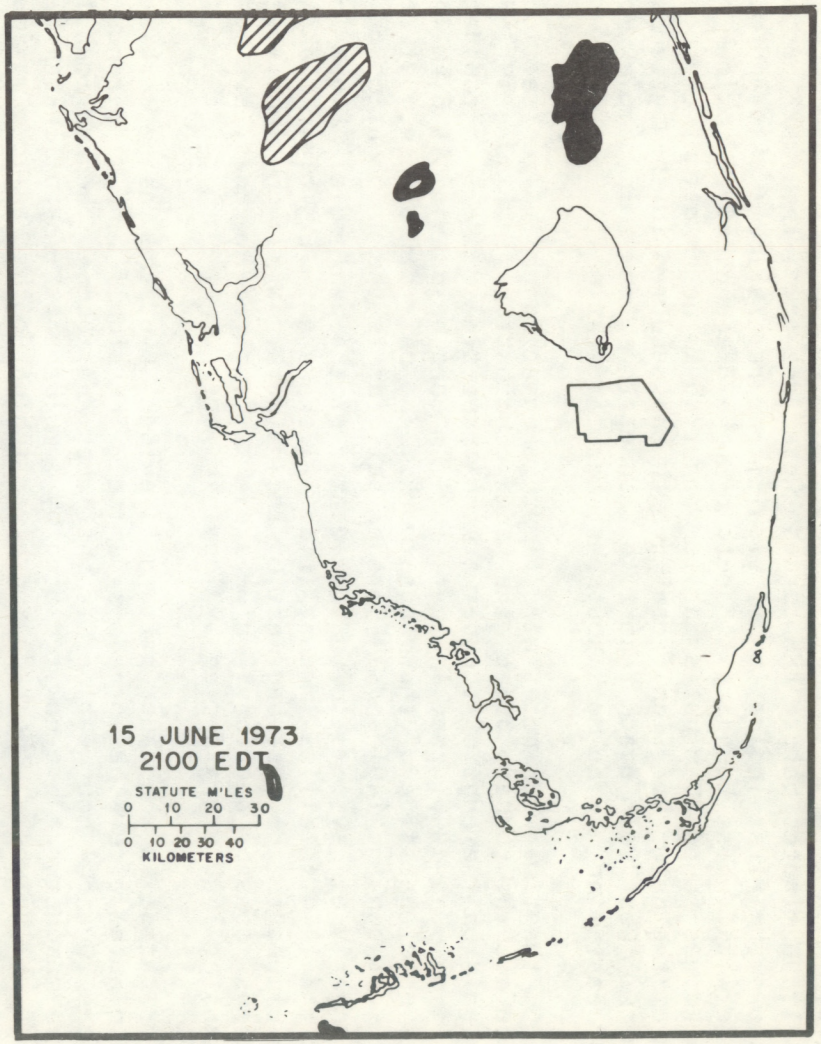

Figure 24. See extended caption, page 21.

At 1401, 90 minutes before the tornado was first seen, the radar pattern (fig. 18) shows the first indication of significant rain systems east and west of the mesonetwork, whose boundary is south of Lake Okeechobee. A maximum echo top of 15.6 km was found 20 minutes earlier about 40 km northwest of the northwest corner of the network. Significant growth has occurred in the system east of the network. West Palm Beach reports a thunderstorm from this complex, but maintains an east wind, as do most southeast coastal stations.

At 1500, the time when notes were first taken at Central Site (section 2), and ½ hour before the tornado began, the radar echo pattern in figure 19 indicates heavy rain on the edge of the network on three sides. Maximum top data are available only at 1440; they indicate maximum echo heights of 15.6 km in the rain systems on either side of the mesonetwork. The only difference, but it is significant, between the 1401 and 1459 radar patterns is the propogation or movement of nearly all systems toward the center of the peninsula. Close inspection of the 1454 satellite imagery (fig. 14) shows a small, clear area between the clouds to the east and west of the network. Winds continue easterly at the southeast coastal stations, which are away from radar echoes, but most other stations at 1500 are affected by local showers.

A major change in the radar pattern is evident over the mesonetwork at 1557, or 17 minutes after the tornado's demise. The significant difference between figure 20 and 1 hour earlier is that the radar echoes then surrounding the echo-free mesonetwork are now replaced by a major north-south line through the middle of the network. The radar observer indicated that an echo maximum was located in the line through the mesonet, but its value was not measured. A top of 16.2 km was measured in the echo southeast of the mesonet at 1540. In general, a major rearrangement of the echo pattern south of the Lake has occurred from 1459 to 1557 that is quite remarkable. Large isolated areas of rain have virtually disappeared from the southwest coast, and a newly organized north-south line over 180 km long has taken its place further east by 1557. Details of this hour's radar events around the network are in the next section. Easterly winds are still seen at southeast coastal stations.

One hour later at 1700 (fig. 21) the location of the radar echoes remains nearly unchanged, but most areas have reduced in intensity to only level 1 or 2, indicating that stratification and anvil cloudiness are dominating. False echo due to anomalous propogation on the eastern side of the echo area has become a problem. The radar observers detected the eastern edge by raising the antenna; verification is shown in part by the lack of rain at coastal stations. A maximum top of 16.5 km was measured on the west side of the line west of Fort Lauderdale at 1635. Recall that the satellite data at 1643 (fig. 14) showed a nearly solid cloud mass over south Florida. Most interesting is the row of stations along the southeast coast now reporting westerly winds at 1700. Coincident with the stratification of the radar echoes during the preceding hour is the reversal from east to west of the southeast coastal winds. This reversal probably represents inflow to the active clouds at 1600 changing to outflow from the stratified clouds at 1700. In addition, temperatures lowered at these stations in the last hour.

By 1800, figure 22 shows that the rain area has enlarged, mainly toward the west. The echo boundary near the east coast, determined by the radar observer, may not be accurate because of anomalous propogation and the presence of

rain at coastal stations. A top of 14.0 km was measured near the southeast tip of the mesonetwork at 1740.

An hour later at 1900 (fig. 23) the intensity of the unchanged rain area cannot be determined, but is most likely rather light, considering the light rain and weak westerlies along the east coast.

Two hours later at 2100 (fig. 24) the rain south of Lake Okeechobee has disappeared, and echoes are seen only in the Keys and north of the Lake. Winds are calm at Key West and three other stations, and other winds are generally less than 2.5 m s^{-1}. From these final hours, then, it seems clear that (a) flow is very light at the surface over Florida and (b) the clouds that grew during the day over Florida were not moving significantly in response to any larger scale flow.

Upper air soundings at Miami and Tampa on 15 June are plotted on tephigrams in figures 25 and 26. On figure 25 the winds at 0800 show no velocity over 7 m s^{-1} at either station below 200 mb. There is, of course, no jet stream at 200 mb as in higher latitude tornado situations. Wind directions at the two stations do not correlate well until the 300- to 200-mb layer is reached. This is to be expected because of the weak and frequently transient features on most synoptic charts in figures 9 to 12. The Miami sounding is slightly colder below 500 mb than is Tampa's, and warmer above 500 mb. Miami is moister, in general, below 500 mb than Tampa, and drier above 500 mb.

At 2000 (fig. 26) all winds are again under 8 m s^{-1} and correlate well between the two stations only between 300 and 200 mb. At this time, the Miami sounding is warmer below 500 mb and the same as Tampa above 500 mb. Moisture varies considerably in the vertical at both stations and shows no overall pattern. There is evidence at 2000, and perhaps at 0800, of a dry layer in the region from 850 to 650 mb at Miami. Golden (1974) indicated this to be a frequent feature accompanying Florida Keys waterspouts. Such a dry layer is frequently associated with the trade wind inversion when it reaches Florida.

In terms of stability, the 0800 Miami sounding was analyzed each day during FACE 1973 from 11 June to 12 September. Values are listed by Staff, EML (1974) in terms of the Showalter Index. The 15 June sounding indicated an index of zero; 48% of the days during FACE had an index equal to or less stable than zero, so stability alone does not isolate 15 June as an unusual FACE 1973 day.

Shear, however, was the weakest of the summer. The 850- to 200-mb shear on 15 June was only 1.5 m s^{-1}. Only 15 and 16 June shared such a low value; all other days had greater shear. In fact, 92% of the 11 June to 12 September days had shear over 5 m s^{-1}. The combination of weak flow on the synoptic and Florida scales, with very weak shear, indicates virtually no echo motion on 15 June, which allows the dominant scale to be the sea breeze and thunderstorm circulations.

5. MESONETWORK SCALE

The Thunderstorm Project (Byers and Braham, 1949) studied Florida and Ohio clouds with surface, airborne and radar instrumentation. This project gathered and analyzed the first detailed measurements of many important thunderstorm properties such as cold downdrafts, divergence-convergence patterns, and

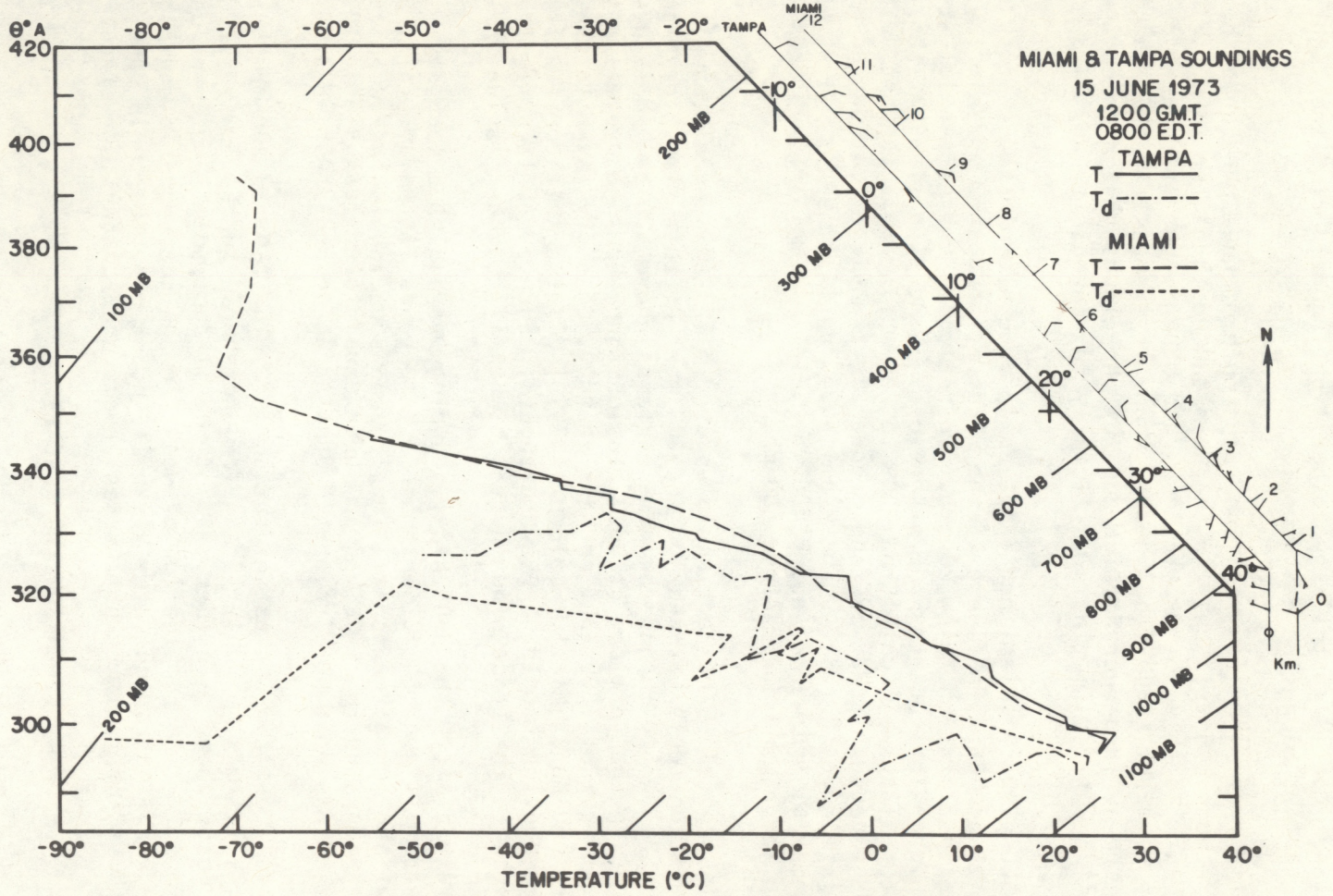

Figure 25. Tephigram plots of temperature and dew point for Miami and Tampa at 0800 EDT on 15 June 1973. On this chart, temperature is constant along the vertical, potential temperature constant in the horizontal, and constant pressure lines are angled as shown. Winds at various levels are plotted to the right with a kilometer scale shown. North is toward the top of the diagram for winds. Full wind barb represents 5 m s^{-1}.

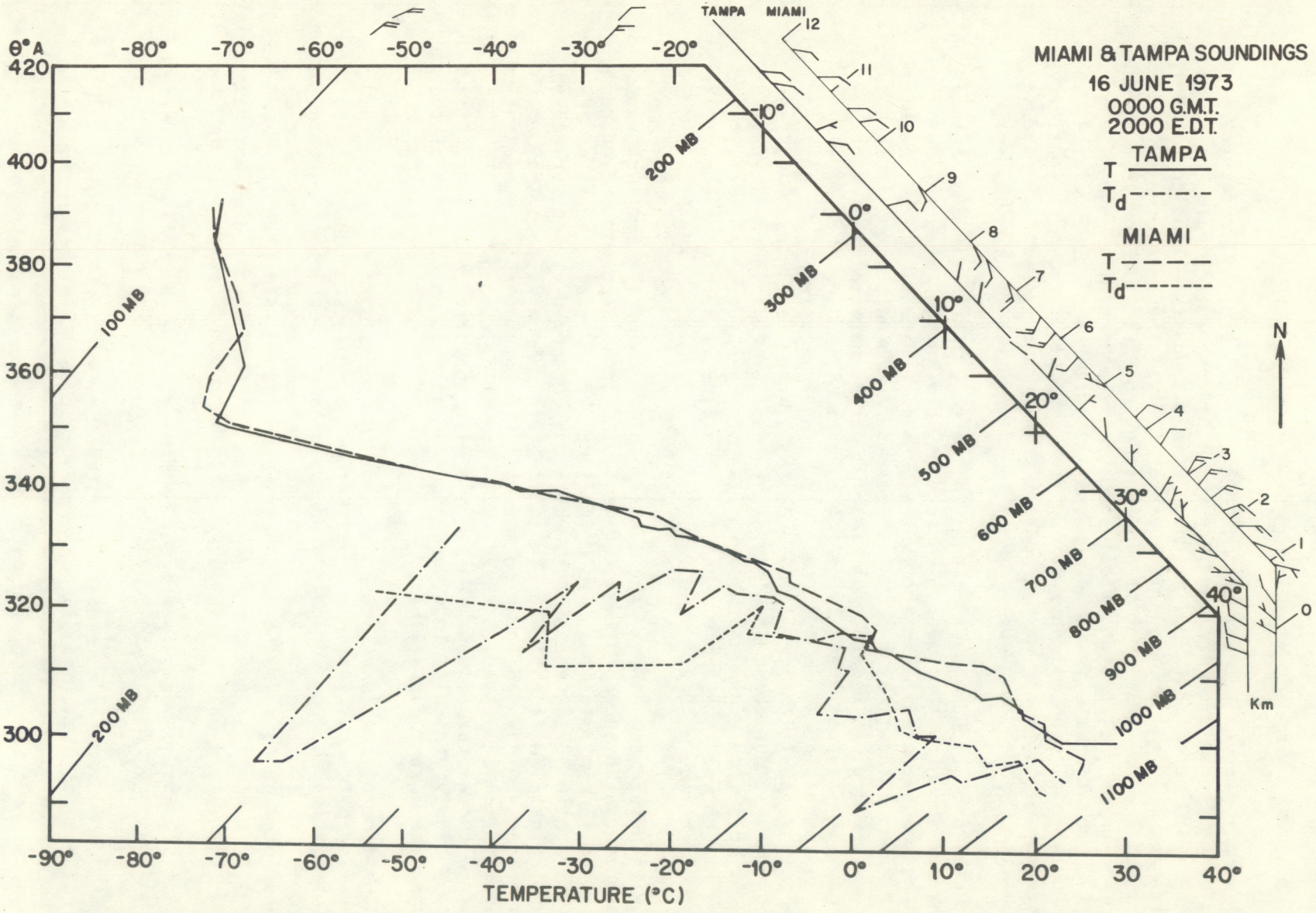

Figure 26. Same as figure 25, except at 2000 EDT on 15 June.

entrainment. The surface networks of FACE in 1971 and 1973 were very similar, and were the largest in Florida since the Thunderstorm Project. Fernandez-Partagas (1973) used FACE 1971 mesonet data to study the relationship between convergence, rainfall and radar echoes for typical thunderstorms on three days. Ulanski, of the University of Virginia, is using FACE 1971 and 1973 information to compile an extensive statistical summary of each rainfall event in the mesonetwork by relating the temporal and spatial patterns of gage rainfall, divergence and vorticity on all days during these two projects. The vorticity and divergence maps to follow were prepared for his research and supplied for this study of the 15 June tornado.

Details of cloud evolution that influence events in the mesonetwork on 15 June are shown by the radar time section in figure 27 over an area about 3 times the mesonet area. The arc is the 50 n.mi. range circle of the Miami WSR-57M radar. The first two contour levels have been omitted to show only major features. This figure amplifies the period between the two hourly Florida radar maps of figures 19 and 20. At the start of the sequence at 1449, clouds with cores exceeding 30 mm hr^{-1} rainfall rate are located 25 km east and west of the tornado position (triangle). By 1532, when the tornado was first photographed, these clouds have dissipated, at least at the higher intensities shown here. At this time a new north-south line of echoes develops near the tornado and halfway between the two old cells. This line is part of the much larger line shown in figure 20.

Within the mesonetwork, the overall influence of the two clouds outside the mesonet can be shown in two east-west wind cross sections indicated in figure 2. The line of stations A to D in figure 28 is located south of the tornado location; station B is Central Site where the tornado pictures were taken, and wind and rainfall were estimated by the authors. From 1450 to 1545, rather strong easterly winds are found on the east side of the network at station D flowing out from the cloud to the east. Meanwhile, strong west winds at station A are from the western cloud. West winds also prevailed at Central Site (station B). Highly variable winds were recorded at station C, south of the tornado and under the parent cloud line.

The line of stations E to H north of the tornado in figure 29 shows a similar wind pattern. Stations E and F show west winds, and H has east winds. Most interesting are the variable wind speeds and directions at station G, which was closest to the tornado (fig. 2). One frequent feature at station G is a tendency for a northerly wind component to dominate. Since it is north of the tornado, this probably represents inflow to the tornado position and may reflect outflow from the radar echo seen just north of the network at 1459 in figure 19.

At 1500 the authors, located at Central Site, noted a large raining cloud complex from north to west to south, and sighted several dust devils.

Figure 30 shows the mesonetwork data in detail at 1510, 20 minutes before the first tornado sighting. The observed C-set winds (m s^{-1}) in the upper left show the west wind outflow over the west half of the network from the mature storm in the west, and east wind outflow over the eastern third of the network

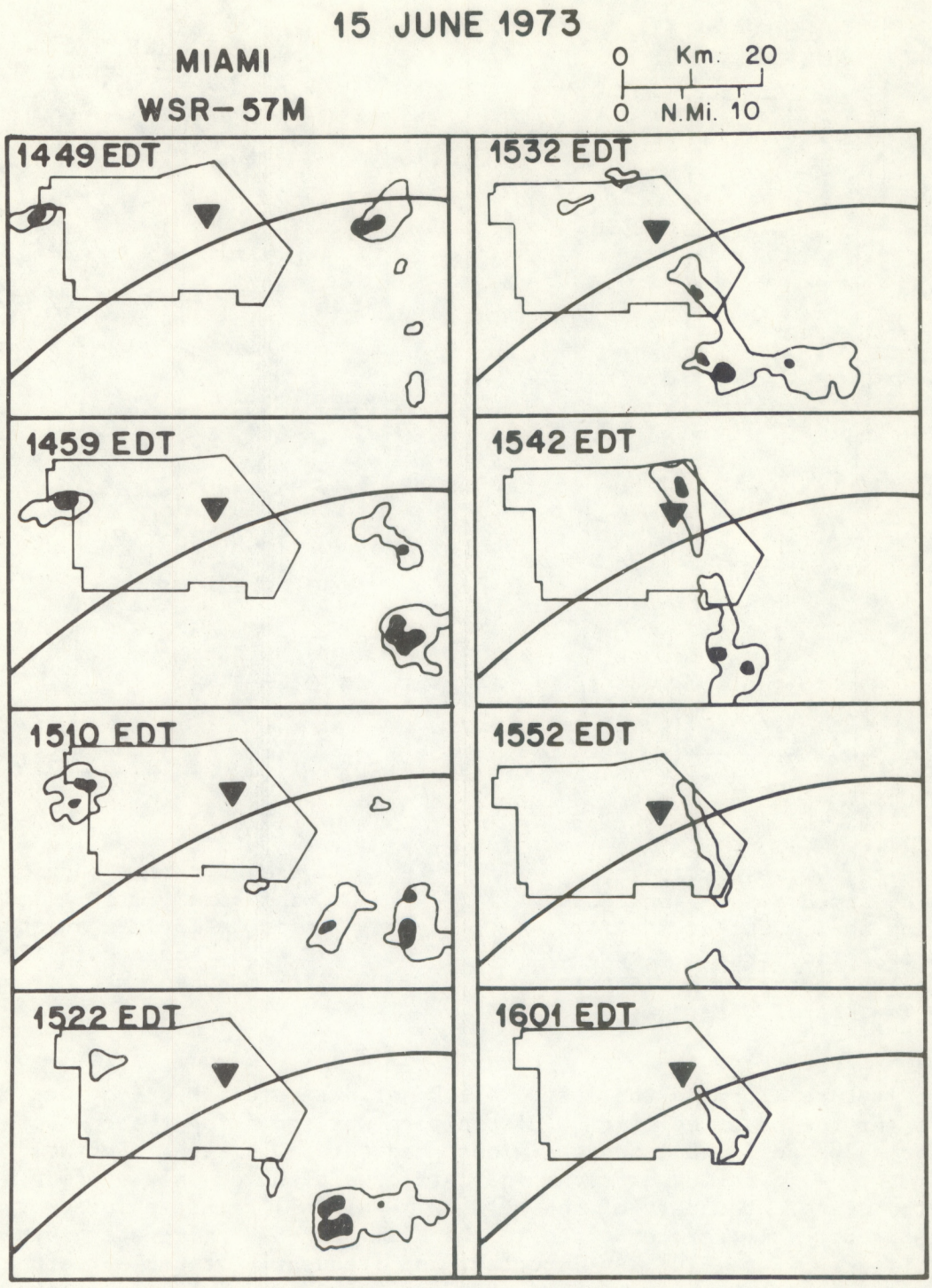

Figure 27. Miami WSR-57M radar data at 8 times on 15 June. The polygonal area is the surface mesonetwork of figures 1 and 2, and 15 to 24. The curving line is the 50 n.mi. range circle from the radar. Triangles locate the tornado. The first two contours are omitted in this figure to show only the major features. The solid line is the 13.7 mm hr^{-1} rain rate contour; the next contour is 30.2 mm hr^{-1} and encloses a black area.

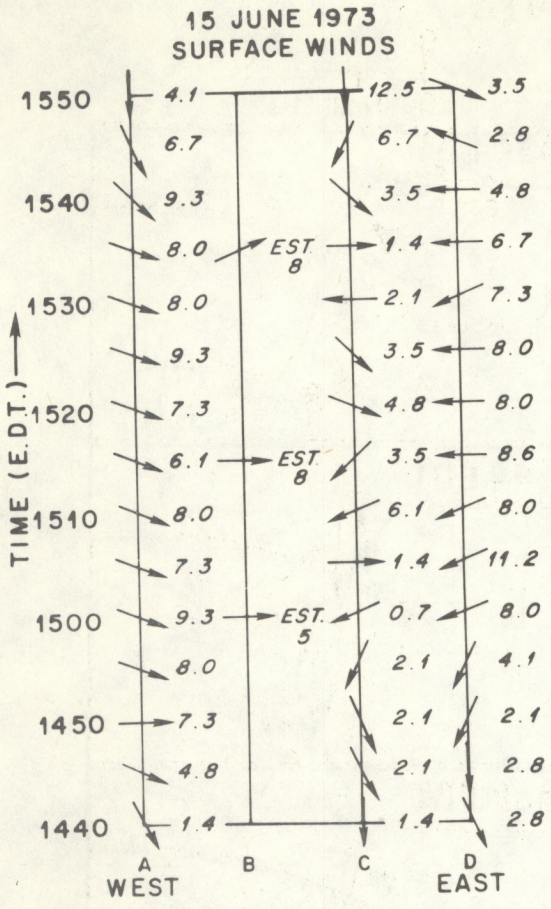

Figure 28. Time section of wind speed (m s^{-1}) and direction on 15 June at stations A to D (located in figure 2) in the mesonetwork. Station B is Central Site.

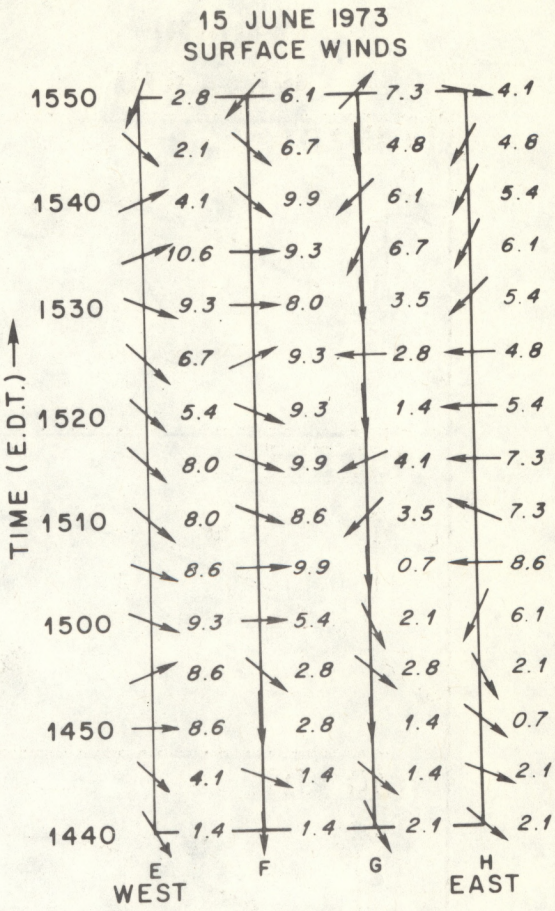

Figure 29. Time section of wind speed (m s^{-1}) and direction on 15 June at stations E to H (located in Fig. 2) in the mesonetwork.

from the mature storm in the east. All C-set data are for a 5-minute period centered at the observed time. This pattern was shown for the rows of stations in figures 28 and 29, but now the widespread nature is seen. Surface rain gage data (mm hr^{-1}) in the upper right indicate precipitation only at four stations along the western boundary of the network. Rainfall rates measured by the Cumulus Group digitizer connected to the Miami WSR-57M radar are given in right center figure 30 at 1510. An important and frequently valuable feature of the digitizer data is the centering of the radar beam near 1.8 km over the network because of the nearly 100-km distance from the radar. The similarity of the precipitation pattern and amounts from both radar and gages on the west side of our area indicates that rain is falling in a relatively continuous shaft from 1.8 km to the surface. Other smaller echoes are detected at MDS (Minimum Detectable Signal) to the north and over 20 mm hr^{-1} to the east. Each of these areas represent rainfall from echoes on the edge of the mesonetwork, as shown in figure 19, but the rain is not reaching the ground. More accurately,

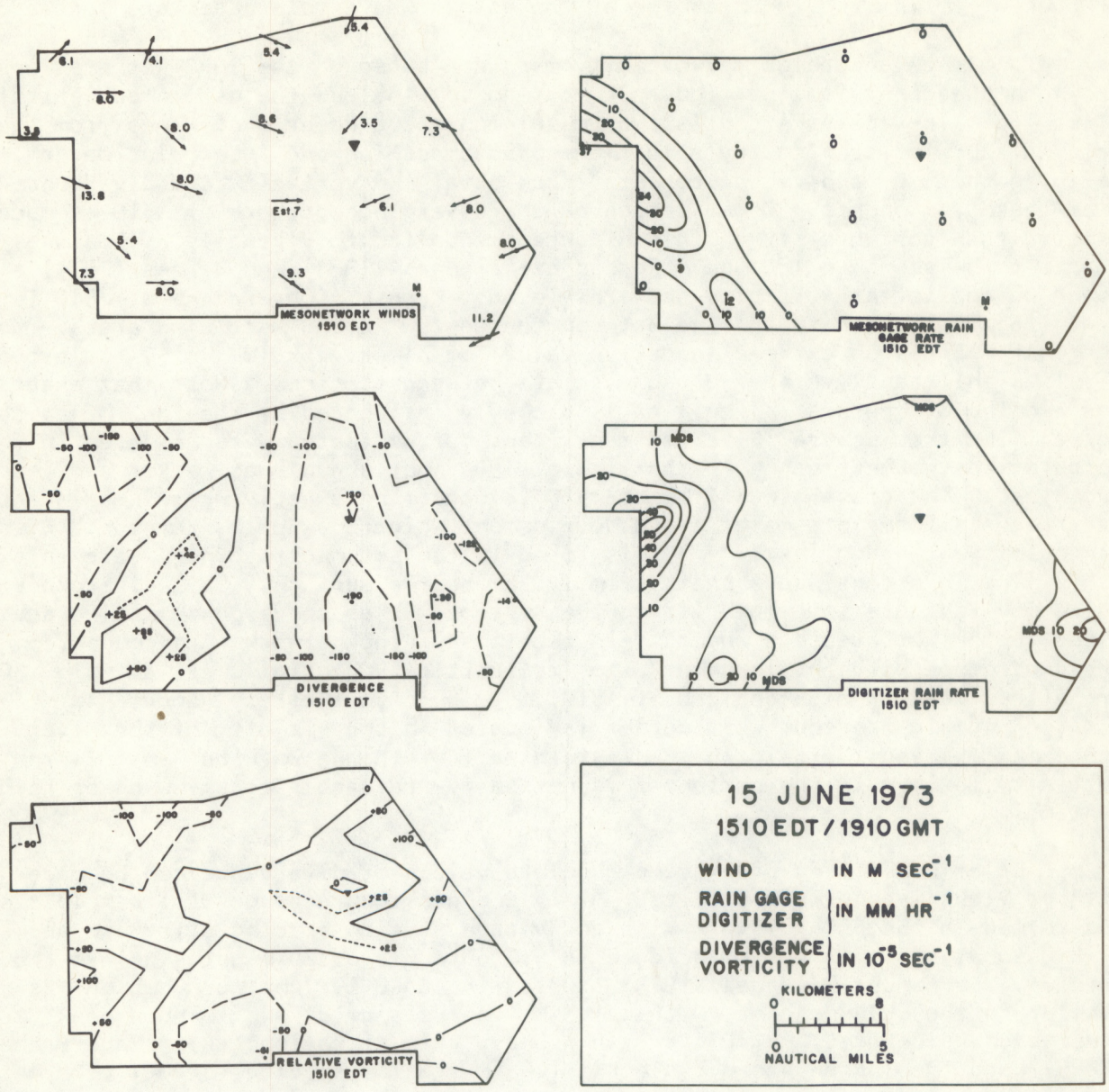

Figure 30. Mesonetwork data on 15 June at 1510. Upper two panels show data measured by the 20 C-set systems. Wind speed in m s^{-1} and rain gage rates in mm hr^{-1}. Central Site values estimated by authors. Divergence and relative vorticity values in 10^{-5} s^{-1} are based on the 20 C-set systems' winds. All of the preceding values are for a 5-minute period centered at 1510. Digitizer rain rate is obtained from the Miami WSR-57M radar connected to the Cumulus Group digitizer located 98 km from the tornado. MDS refers to Minimum Detectable Signal. Data apply to the minute 1510. Outlines of the mesonetwork have been shown in figures 1, 2, 15 to 24, and 27.

no precipitation is being measured at the points where rain gages are located.

Divergence and relative vorticity maps are based on the 20-C set stations shown in the upper left of figure 30, but do not include the estimated Central Site wind. The analysis consists of obtaining a 2.8-km grid of winds from the original 20 wind stations by a multiple-pass smoothing and interpolation scheme, deriving the u and v components, then obtaining vorticity and divergence from these components. Organization of the divergence pattern at 1510 is much greater than for vorticity. This difference applied to virtually all mesonet charts to be shown on 15 June. Fernandez-Partagas (1973) and Barnes (1974) also found no consistent vorticity patterns in most cases. Convergence at 1510 is organized in a north-south line between the east wind and west wind areas. Convergence reaches an extreme (negative value) of almost 2×10^{-3} s^{-1}, but probably is significantly higher at some points between stations. Note that exact positioning of centers in the line is probably influenced by the lack of an observed wind from Central Site; as mentioned, our estimates were not used in the computations. Convergence in the line at 1500 (not shown) was weaker and less organized. The convergence line at 1510 is occurring exactly where subsequent radar echoes form in a major cloud development which spawns the tornado. Divergence somewhat under 1×10^{-3} s^{-1} is found in the southwest corner where rain is falling in a continuous shaft from 1.8 km to the surface. This divergence value may indicate some maturity to the system. Other convergence maxima are found in the northwestern and eastern sections of the network. In comparison to the divergence pattern, large areas of the vorticity chart (lower left fig. 30) are either weak or disorganized at 1510. Cyclonic vorticity of about 1×10^{-3} s^{-1} in the southwest corner is located in the vicinity of the divergence maximum and the rain in the western part of the network but a similar vorticity maximum in the northeast is not easily relatable to any wind or rain system.

A brief comparison of extreme absolute values of divergence can be made with previous mesonetwork studies. At 1510 a peak convergence of 1.8×10^{-3} s^{-1} was formed in the FACE network with an average station spacing of 6.4 km and with an analysis on a 2.8-km grid for a 5-minute period 20 minutes before the tornado. Fernandez-Partagas (1973) studied the FACE 1971 network, which was similar to the 1973 mesonet, with a 1.3-km analysis grid, and found a peak divergence value of 5.0×10^{-3} s^{-1} in a heavy rain situation. Byers and Braham (1949) used the Thunderstorm Project's 1.6-km station spacing for a 1.6-km analysis
storm. Finally, Barnes (1974) shows a maximum divergence value of 3.6×10^{-3} s^{-1} for a tornado passing through the NSSL mesonetwork with an 11-km station spacing and analyzed on a 3.2-km grid. Ours is the weakest peak divergence value of the four studies because the FACE 1973 divergence calculations are based upon a larger station spacing or a larger analysis grid, or both, than all others except those of NSSL. Their largest divergence is only somewhat larger (3.6×10^{-3} s^{-1}) than our peak 15 June value (2.4×10^{-3} s^{-1}), to be seen later. The Oklahoma system is probably a stronger and certainly longer lasting storm than our 15 June case, and their greater divergence for a wider station and grid spacing is not unreasonable.

At 1520 (fig. 31) the wind systems resemble those at 1510. Convergence continues in the meridional line, and now the peak values are found on the north end of the line. Other convergence centers are in the east and northwest

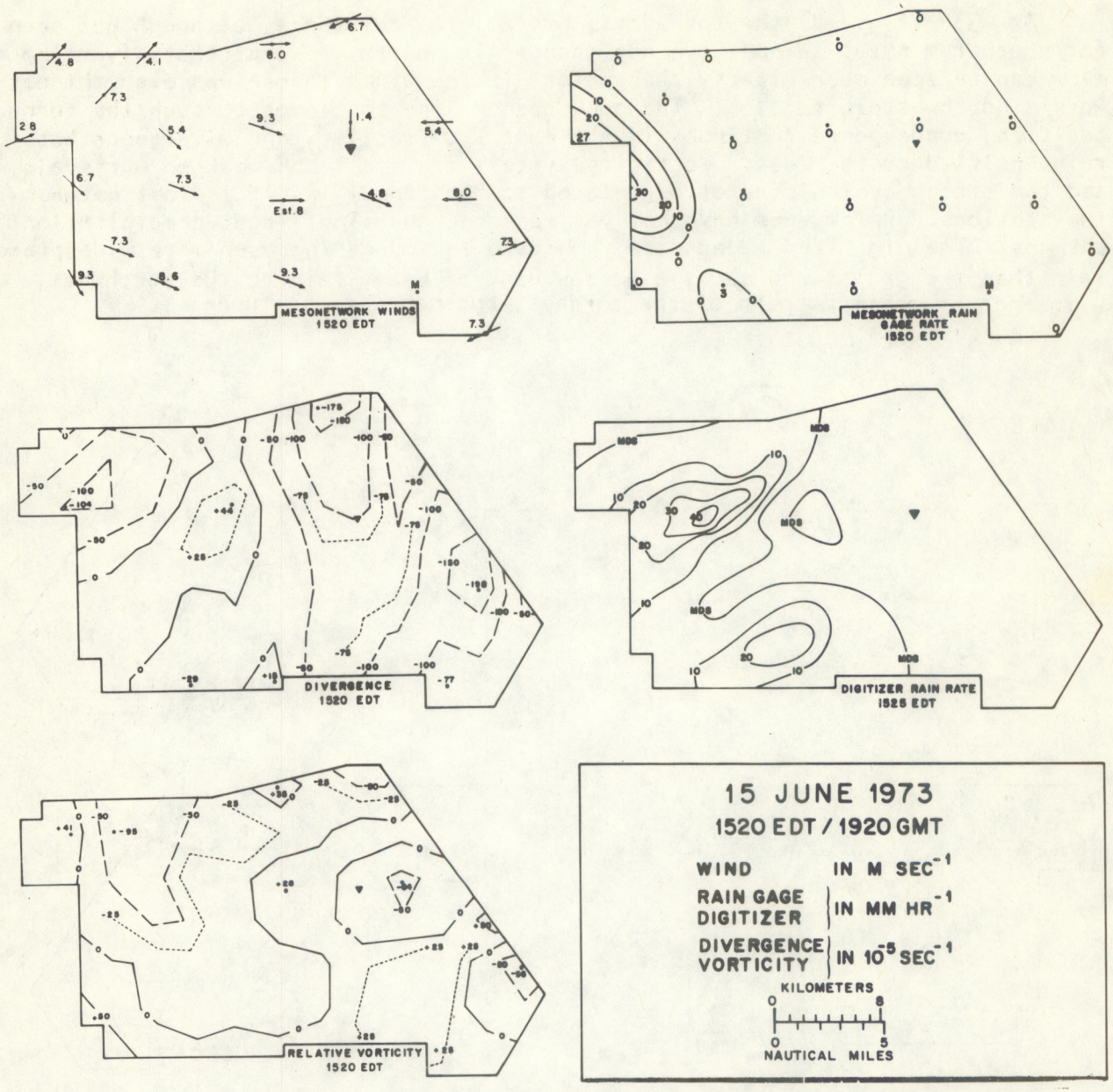

Figure 31. Same as figure 30, except at 1520. Note that digitizer data is at 1525.

sections, as they were 10 minutes earlier. The divergence area in the southwest corner at 1510 is gone. The vorticity chart is fragmented into many transient, small features. Rain gage data are rather unchanged, but the digitizer data at 1525 (none available at 1520) indicates some new developments. The peak rainfall at 1510 was at the western border, but now is further east toward the tornado. Also, the eastern rain center is gone. There has been no "merger" of the eastern and western echoes to form the new cloud line, but the outdrafts have met and formed a new echo line. To an extent, the western line actually has moved and grown eastward to join with the new line, but it does not join with the eastern cloud, since it is gone at 1520 on radar.

At 1530 (fig. 32) the tornado is probably in existence, although not seen for another minute. Winds have not changed in general, except that diverging flow can be seen more clearly than before in the winds themselves over the network's northwestern section. The convergence line continues through the tornado position, convergence continues in the east from earlier, and divergence has reintensified to the west. Vorticity systems are small and weak on our scale, and the strong cyclonic rotation related to the funnel itself is lost between the stations. Rain gages have not yet measured any significant precipitation changes. The digitized radar data, however, is indicating much more widespread rain than the gages, and shows a narrow band of heavy rain to the northwest, with another maximum south of the tornado, but none at the funnel.

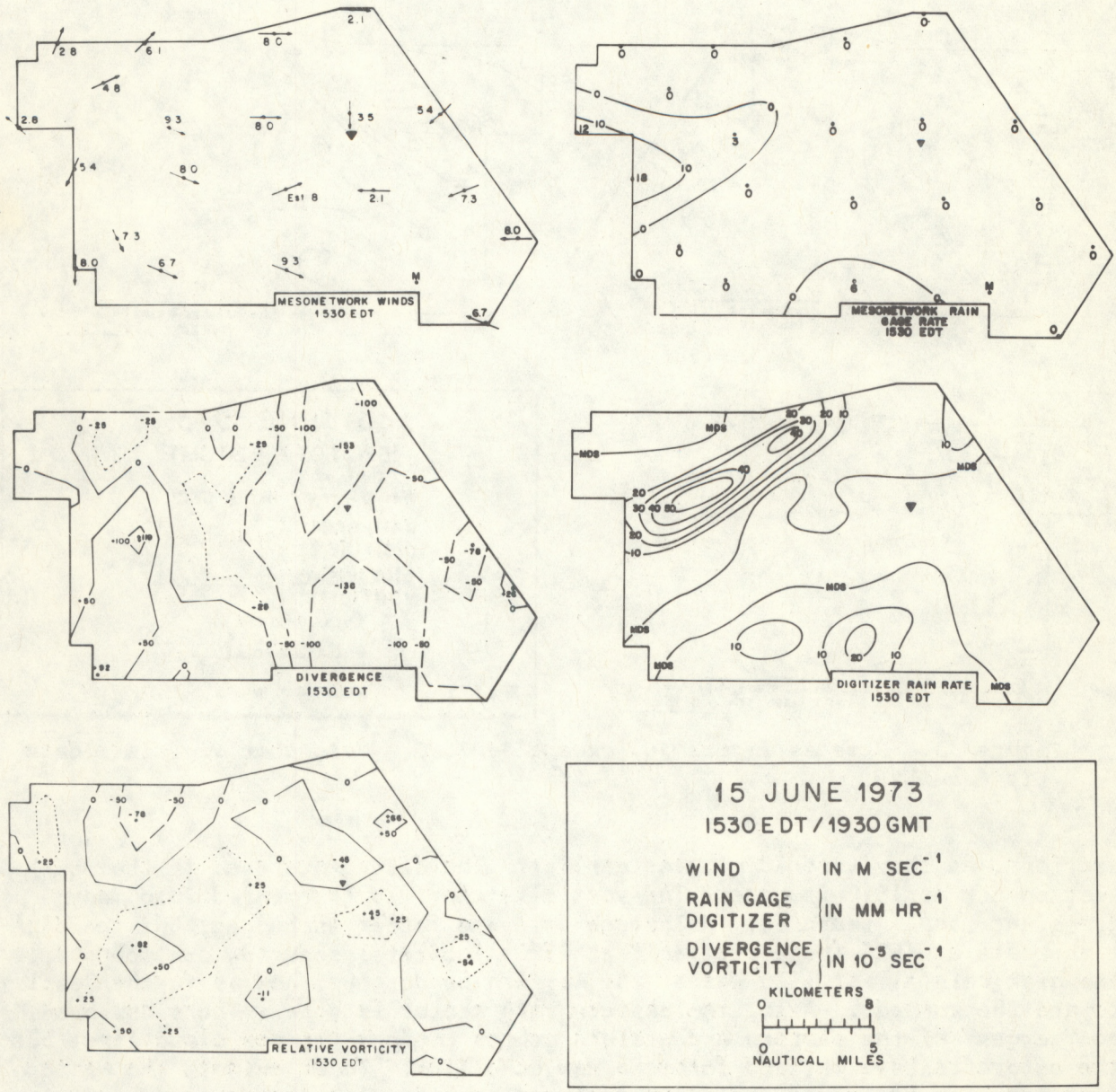

Figure 32. Same as figure 30, except at 1530.

At 1535 (fig. 33), in the middle of the tornado's lifetime, (figs. 4 and 5), winds continue to flow out from the northwestern maximum toward the easterlies. Convergence at the surface has reduced from a long wide line, which in most locations was exceeding 1×10^{-3} s^{-1}, to an isolated center of 2.35×10^{-3} s^{-1} north of the tornado. A divergence maximum is east of the funnel, unrelated to other features. Two strong, but small, vorticity extrema are near the tornado. The rain gages have now measured surface rainfall in a narrow band very similar to the digitizer's line 5 minutes earlier in size, shape, and intensity. The digitizer's band at 1525 still is present, but some indication of a north-south line through the tornado is apparent. Some precipitation is now measured above the tornado.

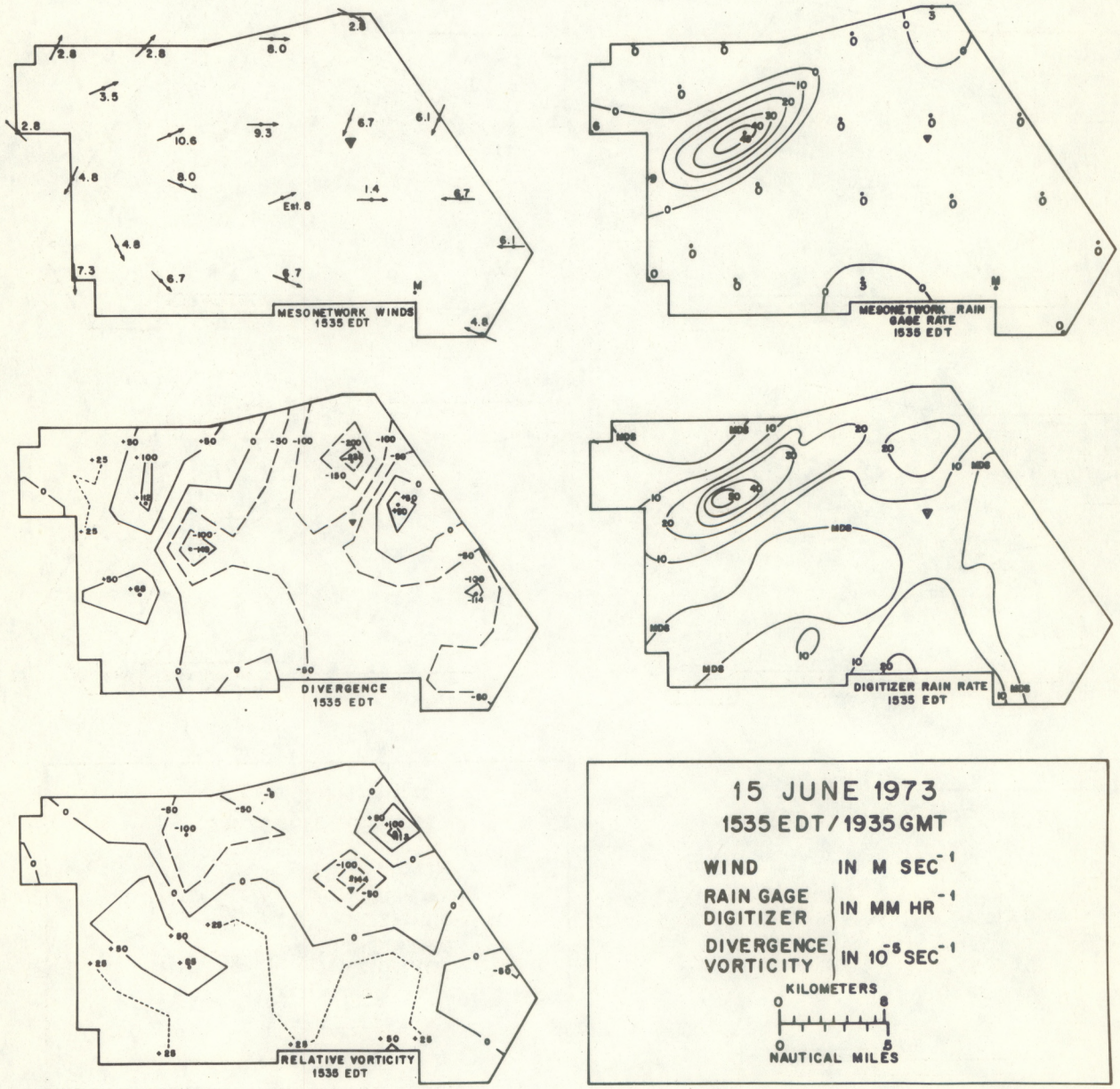

Figure 33. Same as figure 30, except at 1535.

At 1540 (fig. 34), when the tornado was dissipating (fig. 7), precipitation centered at 1.8 km-elevation, as measured by the digitizer, has increased to 20 mm hr^{-1} above the tornado. In addition, rainfall of 18 mm hr^{-1} is reaching the ground only 2 km north of the funnel. These data combined show that rain is falling directly over the tornado at 1540, as was evident in the photographs. Moreover, a north-south line is beginning to dominate the digitizer data while the band to the northwest is decreasing. Rain gages have continued to measure this narrow band, but also show some meridional rainfall in a very similar pattern to the digitizer 5 minutes earlier at 1535. At 1540, when the tornado is dissipating, westerlies are beginning to turn more northerly in the southwest half of the network. Only to the north is there a sufficient westerly

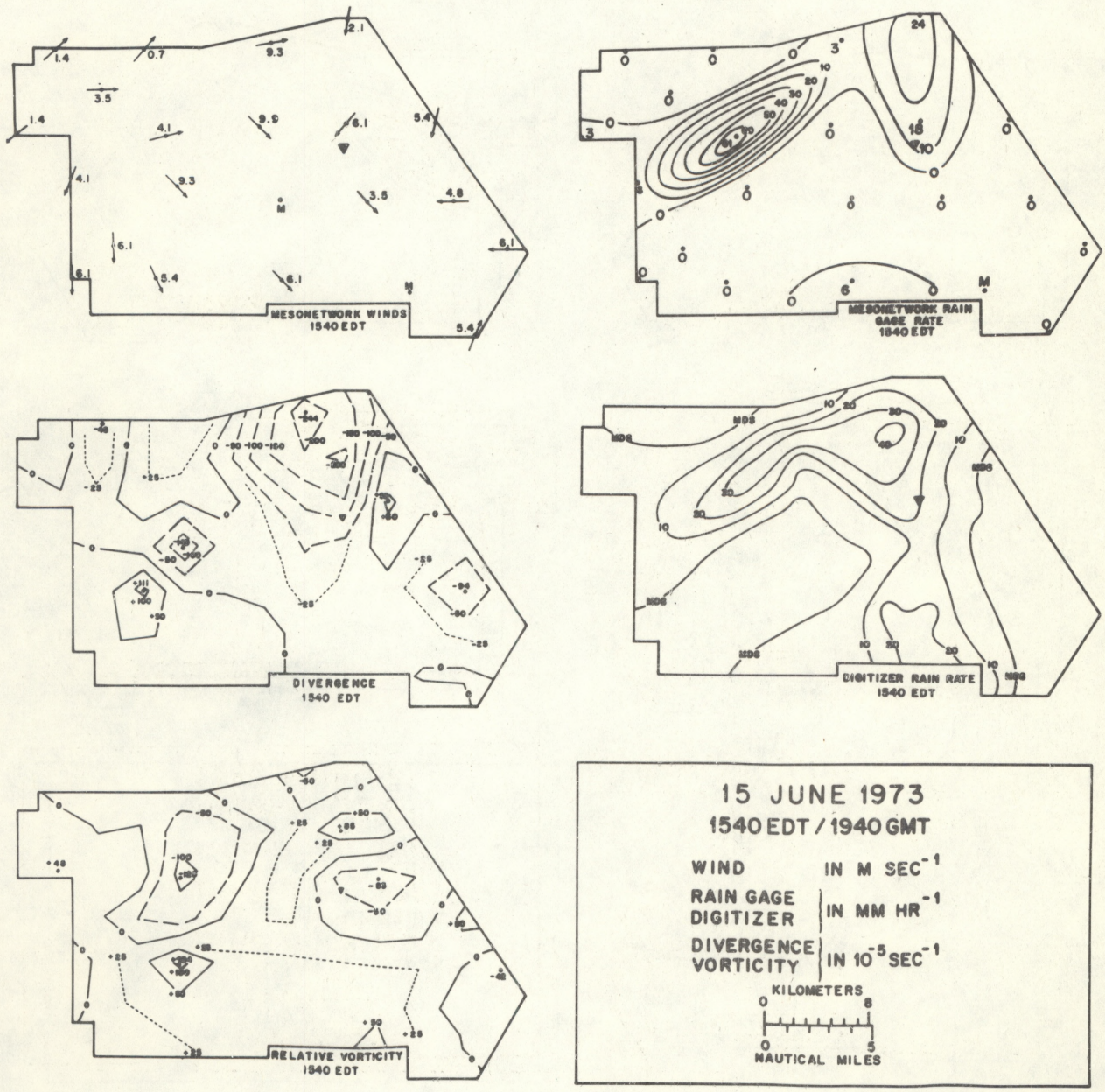

Figure 34. Same as figure 30, except at 1540.

component to cause the day's largest convergence maximum of 2.44×10^{-3} s^{-1}. It is an interesting question as to whether the weakening of the westerlies was the cause of the tornado's demise, or the winds responded to a lack of inflow opportunity when precipitation began to reach the surface. The latter seems preferable, since the convergence had persisted for nearly an hour and had forced a strong updraft which spawned the tornado, but simultaneously carried aloft large quantities of vapor which condensed and had to fall onto the tornado position in the nearly wind-free environment.

At 1545 (fig. 35) the winds are becoming lighter and less clashing in an east-west direction. Convergence is weak, but has not become divergence in

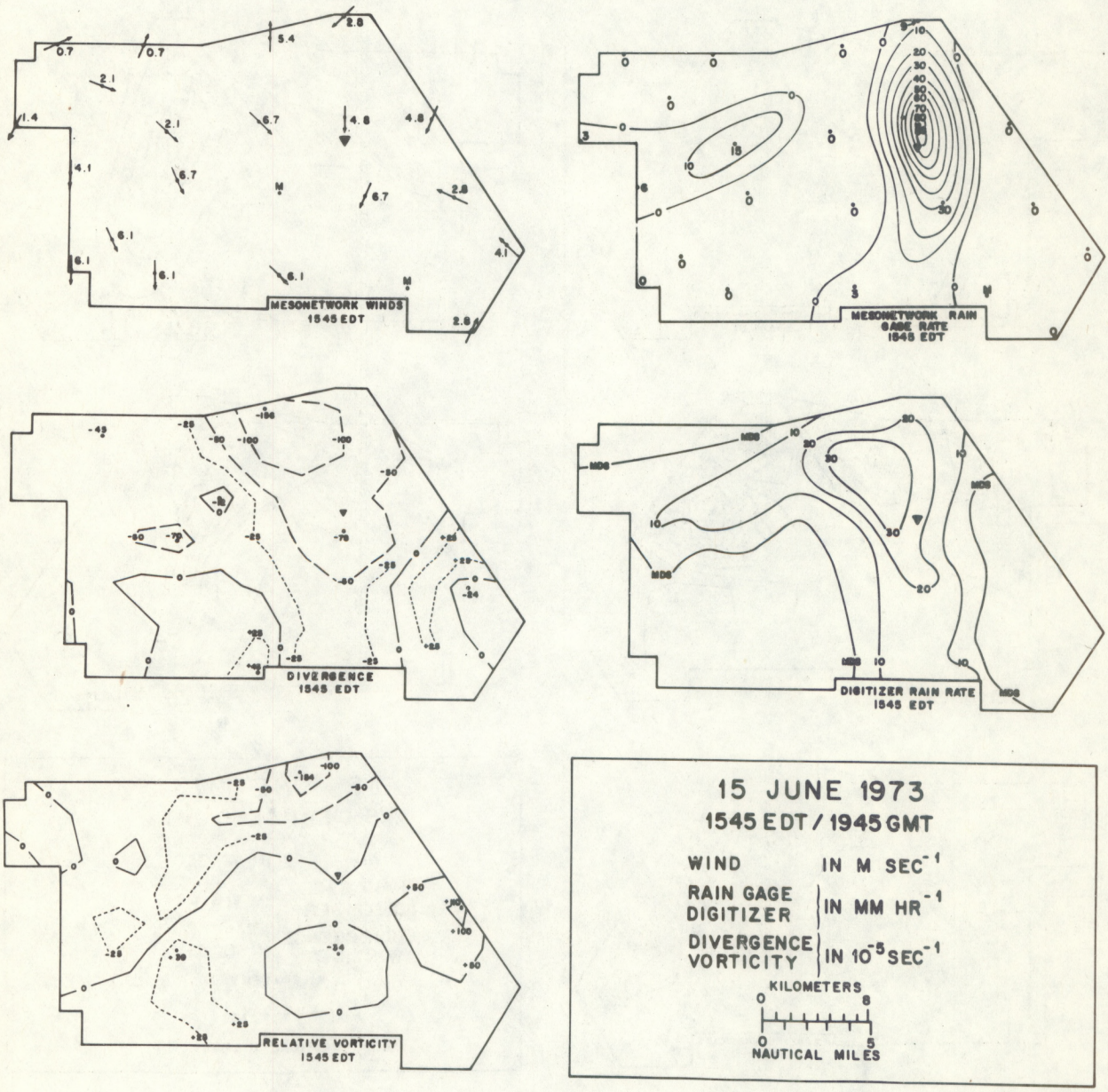

Figure 35. Same as figure 30, except at 1545.

the north-south band through the tornado's former position. The most outstanding parameter at 1545 is the heavy rain just north of the tornado. This rain was pictured in figure 7 at 1542:15. The digitized radar data indicate the same general structure, but the peak is weaker. Differences in intensity probably are due to different systems of measurement, since the rain gage gives a point value compared to the 1° beam diameter of the radar. It is quite remarkable how similar in area and location is this rainfall pattern to the area of convergence at 1510.

At 1550 (fig. 36), heavy rain continues to fall in the meridional line,

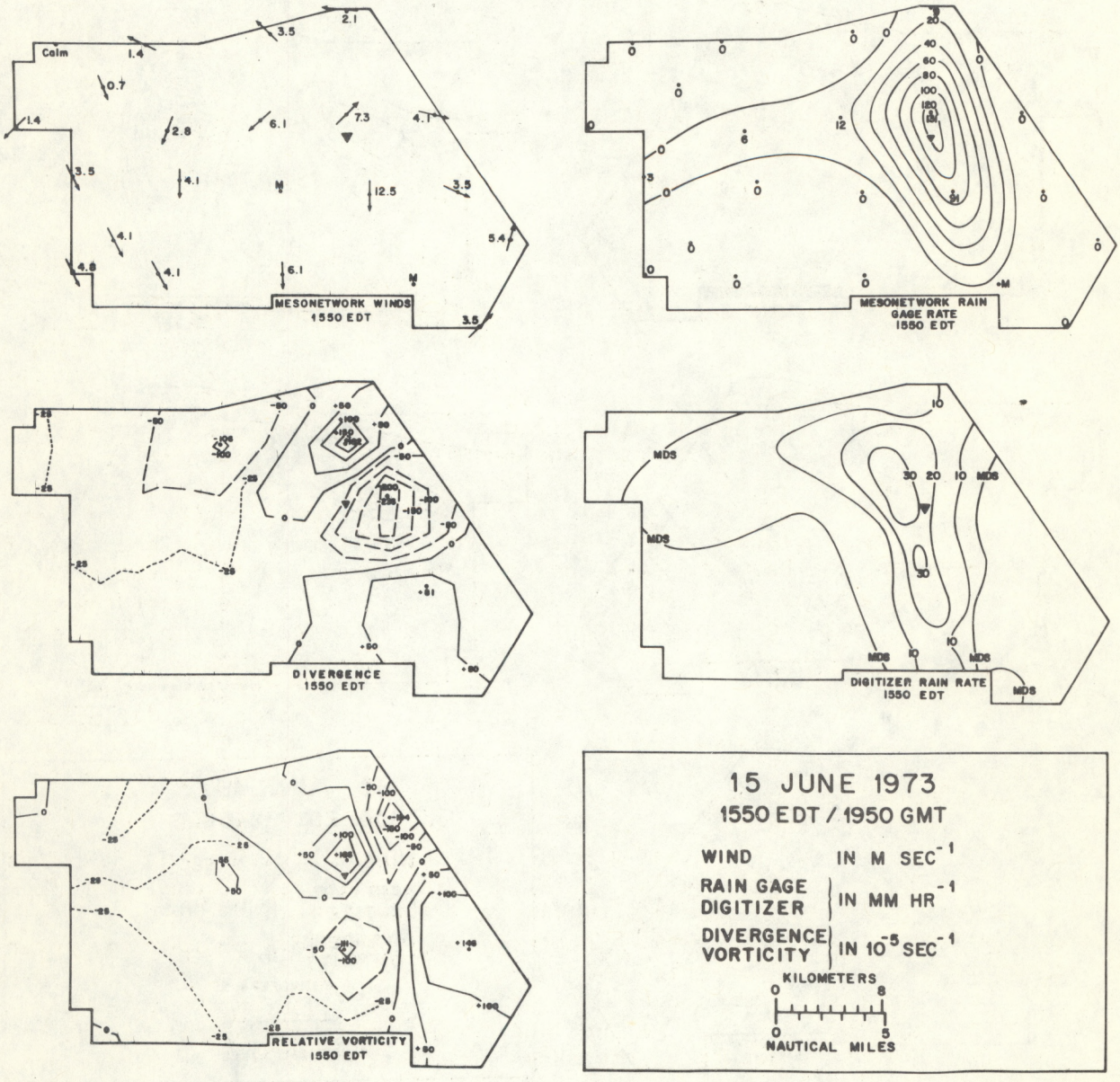

Figure 36. Same as figure 30, except at 1550. Rain gage analysis interval is 20 mm hr^{-1}.

both at the surface and aloft. Nearly all other rain activity is gone. This line is part of a much longer radar line extending the length of south Florida shown a few minutes later in figure 20. Strong convergence is located east of the tornado position and may represent a new cell growing on the east side of the rain shaft. Convergence to the north of the tornado position has become divergence for the first time in the map series. Vorticity extrema continue to appear and then dissipate without any significant continuity or relation to other parameters.

A summary of events in the mesonetwork may be made on the basis of the size and continuity of features. At all times the vorticity pattern was isolated and lacked continuity. Before the tornado formed, the wind and divergence features were strong, well-organized, and covered one-third of the mesonetwork or more. The surface and digitizer rain features were less dramatic, but not transient. When the tornado reached its peak at 1535, the wind and divergence patterns were beginning to lose their widespread characteristics, and the digitizer showed larger rainfall areas with continuity. By the time of tornado dissipation, the rain gage precipitation patterns also were intense and continuous in time. Together with the digitizer patterns, they had replaced wind and divergence as the most revealing parameters.

Physically, developments in the mesonet may be reviewed in the following time sequence. Two large showers reached their maximum activity between 1445 and 1500 (fig. 27) to the east and west of the mesonetwork. Air flowing out from them met near Central Site beginning at 1500, when significant convergence began at the surface along a meridional band. This convergence continued for nearly 40 minutes, and a new cloud grew vertically above the cloud line. A tornado formed under the parent cloud line at 1530, then reached its peak intensity at 1535. At that time the radar began to detect precipitation at the 1.8-km level over the tornado. At 1540 the rain reached the funnel, representing a downdraft where formerly rising air had induced the tornado. The funnel dissipated and was replaced by very heavy rain. The exceptional intensity of the precipitation can be considered indicative of the strength of the original convergence that formed the parent cloud line. Later data, at least those through 1550, do not show a significant downdraft from the tornado-producing cloud.

Reasons for the lack of subsequent downdraft near the funnel during and shortly after tornado dissipation may be found on a somewhat larger scale, such as figure 27. The first convection of the day over south Florida may be called "first generation" cloudiness. It forms where interaction occurs between the prevailing wind flow and the surface heating, the sea breezes and lake breeze, as shown by Pielke (1974). These clouds are not associated with other clouds or connected to them by their anvils. On a calm day, such as 15 June, they form and dissipate *in situ* and generate outflow and divergence on a scale only a few times larger than themselves. Under optimal conditions of spacing, intensity, and vertical wind and thermodynamic conditions, outflows from first generation clouds meet and form second generation clouds, such as the tornado's parent cloud line on 15 June. As the line grows, it is the primary location for new cell and tower growth on the edges and ends, with merging middle and upper level cloudiness. Under such complex conditions, the third generation clouds are formed within, or are directly associated with, clouds composing the line. Actually, an hour later, the entire cloud line system formed a

major organized outdraft which reached the southeast coast by 1700 (fig. 21). Then, it apparently was too late, or in the wrong place, for the outflow to intersect other clouds' drafts and form more clouds.

The entire day's rainfall on 15 June is shown by figure 37. Data for this map consist of values from 229 nonrecording rain gage locations spread at 1-mile (1.6-km) intervals over the mesonetwork. They were typically read during the morning each day. Fortunately, no rain fell on the morning of 15 or 16 June. All precipitation is then related to events on the afternoon of 15 June. With the exception of one station on the northwest edge and one in the southwest corner, all stations had precipitation. Central Site had less than 10 mm, which occurred after 1600. Two distinct features appear: (a) the line to the west consisting of rain that fell mainly from 1455 to 1530; and (b) the north-south line which rained principally between 1540 and 1615. In comparing patterns to the 5-minute values in figure 30 to 36, note that data are not plotted in 5-minute rates in figure 37. Summarized over the afternoon, peak rainfall is in the tornado's parent cloud line which passes directly through the tornado, and is stronger to the south in two locations. The gradient on either side is strong, but not nearly equal to the maximum 1973 daily gradient of 63 mm per km (Woodley et al., 1974).

6. RELATED TORNADO CASES

Two additional tornado situations that may be related to the FACE outflow-interaction tornado should be included here. One case concerns two tornadoes that occurred near Tampa on the same day as the FACE tornado; the other concerns a tornado in Oklahoma. Data for these storms are sparse compared to the FACE mesonetwork study, but some similarities in their structure can be seen.

The first tornado was reported on the hourly teletype observation from Tampa at 1500 on 15 June 1973. The time was 1425 EDT and the location was 20 miles east of Bradenton, or 149° at 59.4 km from the Tampa radar. This public report indicated a lack of deaths or injuries. It may not have been verified, because it did not appear in the monthly publication Storm Data from NOAA, U.S. Department of Commerce. Figure 38 shows this tornado is between two echo lines which are almost stationary for 15 minutes before and after the tornado observation time. In fact, no cloud grows in this position during the next hour, contrary to the FACE tornado just described. This area between the echo lines probably is the site of outdrafts, however, on either side of the reported tornado position. Three reasons can be suggested for a lack of radar echo associated with this tornado report:

1) The position was inaccurate, either in the public report or in the radar picture's azimuth or centering. An error of several km would place the report near the edge of an echo.
2) There really was no tornado, but rather a low cloud base, or chaotic scud clouds, which might have existed between these two lines of echoes.
3) The tornado occurred independently of the rain on the outer edge of the outflow region and had a highly tilted structure while it attempted to maintain connection to an updraft. A similar tilt occurred late in the FACE funnel's lifetime. Additional photographic or observer data would be needed to explain exactly how this tornado occurred in an echoless region.

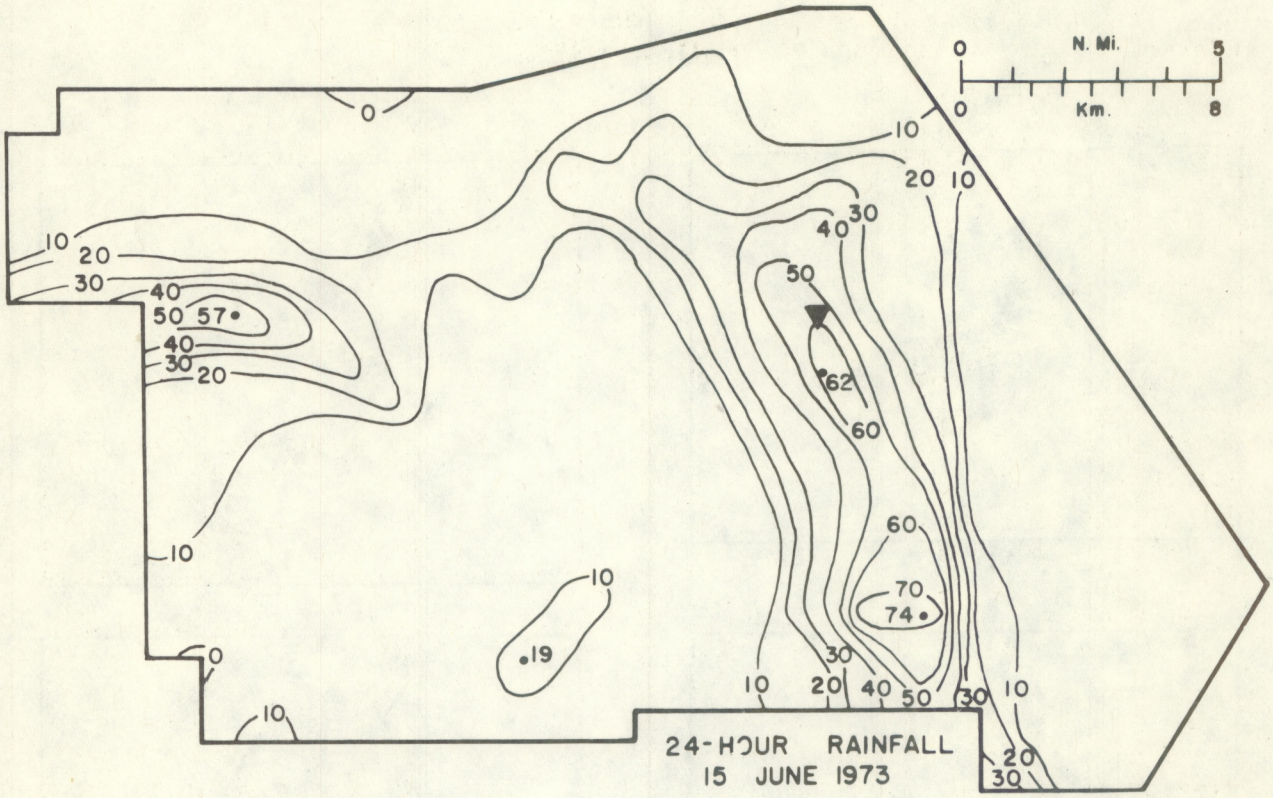

Figure 37. Surface rain gage rainfall from the morning of 15 June to the morning of 16 June. Values in mm.

Another tornado reported by the public on 15 June was located at 1556 EDT near Zephyrhills, which is 048° at 44.5 km from the Tampa radar. According to Storm Data, the tornado touched down briefly and overturned an unoccupied mobile home. This time the radar data in figure 38 shows the tornado's position to be at the end of an echo line which does not move, but grows toward the tornado. Although not a classic hook echo associated with Midwest tornadoes, it is easier to accept a tornado in this position than the other tornado in an echo-free region.

The weak synoptic flow near Tampa was similar to that described in south Florida on 15 June. The Tampa soundings in figures 25 and 26 show no substantial winds. The only difference was that above 500 mb enough weak easterly flow and easterly shear prevailed for clouds to extend some distance to the west over the Gulf of Mexico, as shown in the satellite data of figures 13 and 14.

The outdraft-interaction mechanism described for the FACE tornado may also be related to an Oklahoma tornado's formation, as called to our attention by Dr. Charles Hosler of Pennsylvania State University. The case occurred during July 1961 near Miami, Oklahoma (extreme northeast corner of state). Figure 39 shows three views taken by Dr. Hosler over a period of about 10 minutes. Pictures were taken from a point north of the city, looking southeast. This

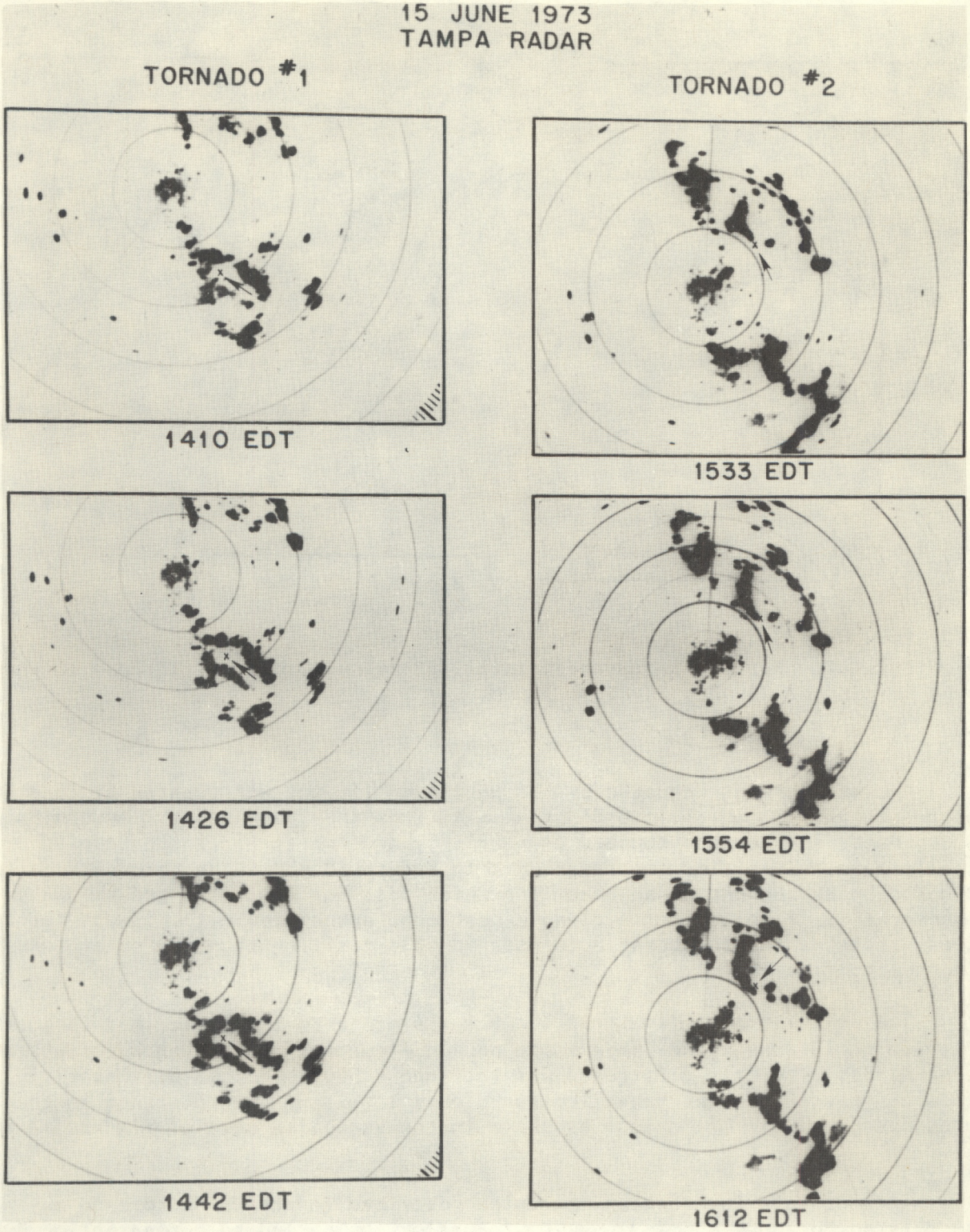

Figure 38. Photographs of the Tampa WSR-57 radar on 15 June. Heavy range circles are 20 n.mi. apart; weak circles occasionally appear at intermediate 10 n.mi. intervals. Each tornado location is shown by an x at the end of the arrow.

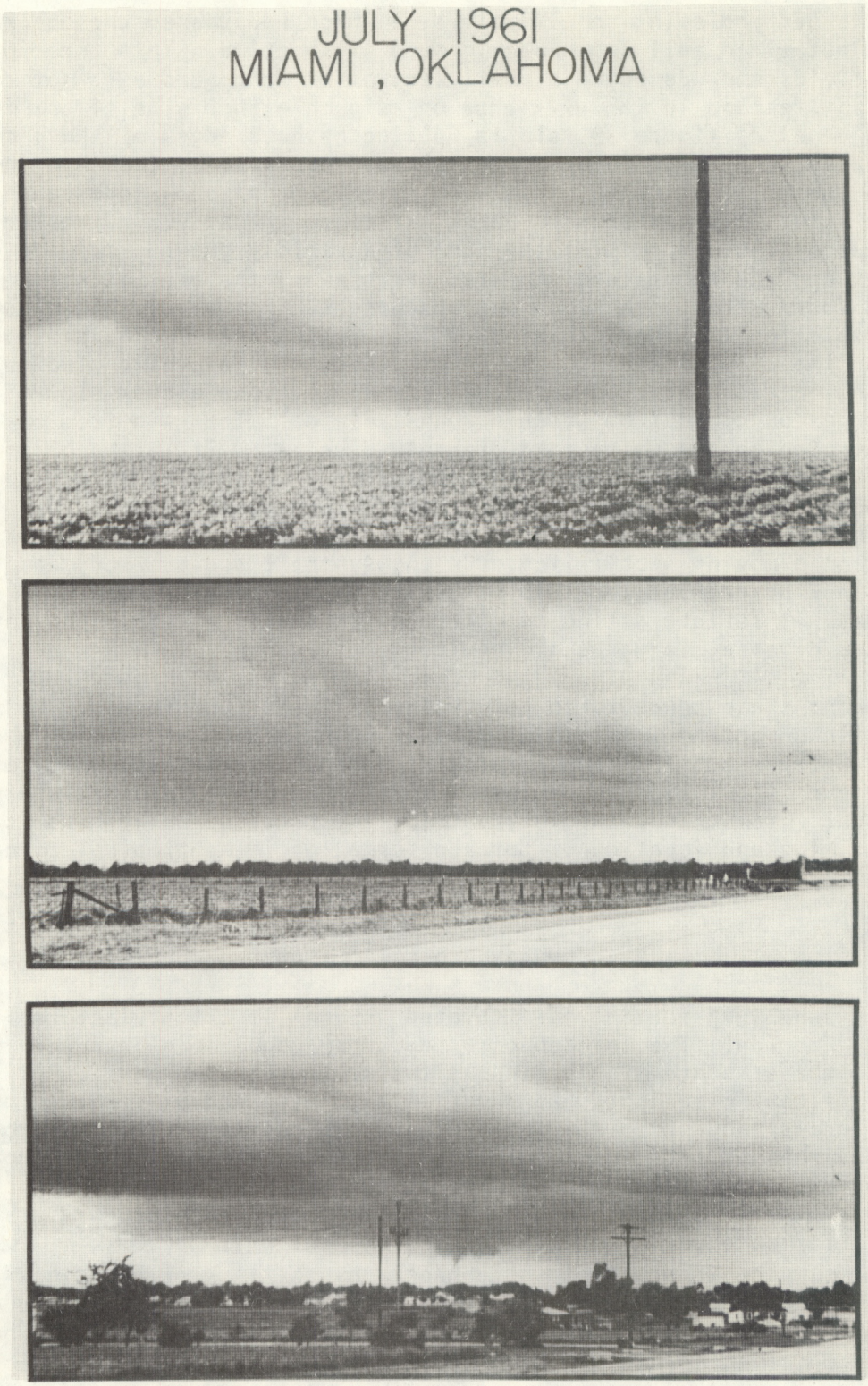

Figure 39. Photographs, taken by Dr. Charles Hosler, Pennsylvania State University, showing a tornado during July 1961 near Miami, Oklahoma. The photos look southeast, perpendicular to a squall line, from a point north of the city.

direction is perpendicular to a squall line which had passed the observation point. Walnut-sized hail was on the ground at the time. This tornado touched down over fields and destroyed a small section of fence and a row of trees. The important feature is the existence of rain on either side of the funnel. In the top panel of figure 39 rain is falling on both edges of the picture. Although it is less evident here, the rain was observed at the time and is visible on the original color slide. The middle panel shows the funnel a short time later, between showers on either side. Finally, Dr. Hosler noted that a pedestal cloud formed at the base of a rapidly-growing cumulus congestus located between the two mature showers. With time, the precipitation shifted toward the vortex from both sides and obscured it from view. The process is nearing completion in lower figure 39. This entire life cycle is remarkably similar, on the cloud scale, to the FACE tornado's life cycle. Two mature showers, in the associated downdrafts, were situated on either side of a new growing congestus cloud from which a funnel dipped. The rain from one of the showers extended to the vortex and probably dissipated it, although the later stages of the tornado were not seen in Oklahoma. While cloud-scale motions may have been similar in the two cases, the larger scale flow is not. In Florida, there was no cloud motion, while in Oklahoma the rain and tornado interacted on a moving squall line. On the synoptic scale, winds and shear were weak in Florida, but were typically strong for squall lines in Oklahoma. Nevertheless, it is interesting to note the similarity of the cloud interactions in two diverse, larger scale environments.

Extending these concepts to the typical mid-latitude tornado, we may have strong outflows meeting from two clouds, as we have seen in Florida and Oklahoma. Or, the outflow from a large cloud may interact with the larger scale low-level flow, such as on the south side of moving storms, where hook echoes occur. From this viewpoint, outflow interaction may help us to understand the timing and location of tornado formation in nontropical tornadoes.

7. SUMMARY AND CONCLUSIONS

The 15 June 1973 tornado has isolated several important factors in cloud growth over Florida. The tornado occurred under conditions that were nearly opposite to the standard mid-latitude situation. There were virtually no shear and no significant cloud motions. Neutral stability and only weak trough conditions prevailed. Over the peninsula, a typical cloud evolution occurred for this environment. Clouds formed from the sea breezes along the coasts and moved slowly inland. Other clouds were associated with the Lake Okeechobee lake breeze. The interaction of downdrafts from two large clouds outside the mesonetwork formed a new cloud line in the mesonet half way between the original thunderstorms. The interaction was enhanced by the lack of any significant wind flow. As the new line grew rapidly in response to the surface convergence of nearly 2×10^{-3} s^{-1} for one-half hour, a funnel dipped from the line and the tornado was observed for 10 minutes. Rainfall was detected by the digitized radar, whose beam was about one km above the tornado at its peak intensity. Rain then reached the funnel 5 minutes later to cause its dissipation. Within 5 minutes after the tornado's demise, extremely heavy rain was being detected by the rain gages. This was associated with the downdraft, which replaced the updraft spawning the tornado.

There were other tornadoes near Tampa on 15 June. One was near the end of a long radar echo, but the other occurred in an echo-free area, for unexplained reasons. A tornado photographed on a squall line in Oklahoma occurred between two rain showers that gradually moved toward the vortex in a manner very similar to the FACE tornado, suggesting the importance of downdraft interaction in this situation also.

We conclude that outdraft interaction between strong, antecedent clouds can form intense new clouds which spawn tornadoes during weak flow conditions in Florida. The convergence pattern related to the antecedent clouds' outflow is much better organized and stronger than the vorticity pattern on the mesoscale. When precipitation appears above the funnel, which forms under the cumulus updraft, it signals the reversal to downdraft in the cloud, and the tornado dissipates when the downdraft rain reaches it. This life cycle is very similar to that of the Florida Keys waterspout. Other tornadoes in Florida occur in moving squall lines during winter and spring, or are associated with tropical disturbances. But the cloud interaction mechanism on 15 June is possibly vital to many of the short-lived tornadoes that occur in Florida and other tropical countries during the moist season. This little-studied feature is not a miniature mid-latitude tornado related to the usual moving squall line in a strongly sheared environment, but owes its existence to the strength of the tropical cumulus updraft and to the cloud-scale or mesoscale flow. Future studies of data from FACE field programs in 1971, 1973, and 1975 should bring more understanding of the significance of outflow interaction and its role in the growth of merging clouds, both natural and seeded.

8. ACKNOWLEDGMENTS

Several people deserve special mention for making data available for this study. Dr. Michael Garstang of the Department of Environmental Sciences, University of Virginia directed the field phase of FACE 1973; we are especially grateful to him and the staff who accomplished the difficult job of data collection. Stan Ulanski, of the same department, made the divergence and vorticity calculations for the mesonetwork on 15 June. Victor Wiggert, Cumulus Group, NHEML, supplied the digitized radar data for the mesonetwork. Dr. Charles Hosler, of Pennsylvania State University, provided the pictures and observations of the Oklahoma tornado.

Mark Zimmer, National Hurricane Center, NOAA, Coral Gables, patiently explained details of the NHC synoptic charts. Cecilia Griffith, Cumulus Group, NHEML, obtained some of the satellite data on 15 June.

Paul Hannum drafted the figures, Charles True made the photographic prints, and Mrs. Lois Clark typed the various drafts of the text. We express our thanks to all of these NHEML employees who contributed so much to the study.

9. REFERENCES

Barnes, S. L., Ed. (1974): Papers on Oklahoma thunderstorms, April 29-30, 1970. NOAA Tech. Memo. ERL NSSL-69, National Oceanic and Atmospheric Administration, U.S. Dept. of Commerce, Coral Gables, Fla., 233 pp.

Brandli, H. W. and J. W. Orndorff (1976): Satellite-viewed cloud lines, anomalous or others. Mon. Wea. Rev., 104, 210-213.

Byers, H. and R. R. Braham (1949): The Thunderstorm. (Report of the Thunderstorm Project). Washington, D.C., 287 pp.

Chagnon, S. A. and J. W. Wilson (1971): Record severe storms in a dense meteorological network. Weatherwise, 24, 152-163.

Charba, J. (1974): Application of gravity current model to analysis of squall-line gust front. Mon. Wea. Rev., 102, 140-156.

Fernandez-Partagas, J. J. (1973): Subsynoptic convergence-rainfall relationships based upon 1971 south Florida data. NOAA Tech Memo. ERL WMPO-9, National Oceanic and Atmospheric Administration, U.S. Dept. of Commerce, Coral Gables, Fla., 76 pp.

Fujita, T. (1960): A detailed analysis of the Fargo tornadoes of June 20, 1957. U.S. Weather Bureau Research Paper No. 42, 67 pp.

Gerrish, H. P. (1967): Mesoscale studies of instability patterns and winds in the tropics. Final report of Radar Meteorological Laboratory, University of Miami to U.S. Army Electronics Command. Tech. Rpt. ECOM-00443-F.

Gerrish, H. P. (1969): Intersecting fine lines and a south Florida tornado. Preprints Conf. on Severe Local Storms, Chicago, Ill., Amer Meteor. Soc., 188-191.

Golden, J. H. (1974): The life cycle of Florida Keys' waterspouts. Part I. J. Appl. Meteor., 13, 676-692.

Hoecker, W. H., R. G. Beebe, D. T. Williams, J. T. Lee, S. G. Bigler and E. P. Segner (1960): The tornadoes at Dallas, Texas, April 2, 1957. U.S. Weather Bureau Research Paper No. 41, 175 pp.

Holle, R. L. and M. W. Maier (1974): Development of a Florida tornado related to downdraft interaction. Preprints Conf. on Cloud Physics, Tucson, Ariz., Amer. Meteor. Soc., 453-458.

Hoxit, L. R. and C. F. Chappell (1975): Tornado outbreak of April 3-4, 1974; synoptic analysis. NOAA Tech. Report ERL 338-APCL 37, National Oceanic and Atmospheric Administration, U.S. Dept. of Commerce, Coral Gables, Fla., 48 pp.

Lemon, L. R. (1974): Interaction of two convective scales within a severe thunderstorm: a case study. NOAA Tech Memo. ERL NSSl-71, National Oceanic and Atmospheric Administration, U.S. Dept. of Commerce, Coral Gables, Fla., 16 pp.

Maier, M. W. and H. W. Brandli (1973): Simultaneous observation of tornado, waterspout and funnel cloud. Weather, 28, 322-327.

McNeil, G. T. (1954): Photographic measurements: problems and solutions. Pitman Publishing Co., New York.

Novlan, D. J. and W. M. Gray (1974): Hurricane-spawned tornadoes. Mon. Wea. Rev., 102, 476-488.

Pielke, R. A. (1974): A three-dimensional numerical model of the sea breezes over south Florida. Mon. Wea. Rev., 102, 115-139.

Rossow, V. J. (1970): Observations of waterspouts and their parent clouds. NASA Tech Note D5854, Washington, D. C., 63 pp.

Senn, H. V., C. L. Courtright and H. W. Hiser (1969): Preliminary characteristics of south Florida tornadoes in the summer of 1968. Preprints Conf. on Severe Local Storms, Chicago, Ill., Amer. Meteor. Soc., 192-196.

Staff, Experimental Meteorology Laboratory (1974): 1973 Florida Area Cumulus Experiment (FACE) operational and preliminary summary. NOAA Tech. Memo. ERL WMPO-12, National Oceanic and Atmospheric Administration, U.S. Dept. of Commerce, Coral Gables, Fla., 254 pp.

Wise, C. W. and R. H. Simpson (1971): The tropical analysis program of the National Hurricane Center. Weatherwise, 24, 164-173.

Woodley, W. L., A. Olsen, A. Herndon and V. Wiggert (1974): Optimizing the measurement of convective rainfall in Florida. NOAA Tech. Memo. ERL WMPO-18, National Oceanic and Atmospheric Administration, U.S. Dept. of Commerce, Coral Gables, Fla., 99 pp.